

Volume, effusion rate, and lava transport during the 2021 Fagradalsfjall eruption: Results from near real-time photogrammetric monitoring

Gro Birkefeldt Møller Pedersen¹, Joaquin M. C. Belart², Birgir V. Óskarsson³, Magnus Tumi Gudmundsson¹, Nils Benjamin Gies⁴, Thórdís Högnadóttir¹, Ásta Rut Hjartardóttir⁵, Virginie Pinel⁶, Etienne Berthier⁷, Tobias Dürig¹, Hannah Iona Reynolds¹, Christopher W. Hamilton⁸, Gumundur Valsson⁹, Páll Einarsson¹, Daniel Ben-Yehoshua¹, Andri Gunnarsson¹⁰, and Björn Oddsson¹¹

¹University of Iceland

²National Land Survey Iceland

³Icelandic Institute of Natural History

⁴University of Bern

⁵Institute of Earth Sciences, University of Iceland

⁶ISTerre- IRD- Université Savoie Mont-Blanc- CNRS

⁷CNRS

⁸The University of Arizona

⁹National Land Survey of Iceland

¹⁰National Power Company

¹¹The Department of Civil Protection and Emergency Management

November 24, 2022

Abstract

The basaltic effusive eruption at Mt. Fagradalsfjall began on March 19, 2021, ending a 781-year hiatus on Reykjanes Peninsula, Iceland. By late September 2021, 32 near real-time photogrammetric surveys were completed using satellite and airborne images, usually processed within 3–6 hours. The results provide unprecedented temporal data sets of lava volume, thickness, and effusion rate. This enabled rapid assessment of eruption evolution and hazards to populated areas, important infrastructure, and tourist centers. The mean lava thickness exceeds 30 m, covers 4.8 km² and has a bulk volume of $150 \pm 3 \times 10^6$ m³. The March–September mean effusion rate is 9.5 ± 0.2 m³/s, ranging between 1–8 m³/s in March–April and increasing to 9–13 m³/s in May–September. This is uncommon for recent Icelandic eruptions, where the highest discharge usually occurs in the opening phase.

Volume, effusion rate, and lava transport during the 2021 Fagradalsfjall eruption: Results from near real-time photogrammetric monitoring

Gro B. M. Pedersen^{1*}, Joaquin M. C. Belart^{2,3}, Birgir Vilhelm Óskarsson⁴, Magnús Tumi Gudmundsson¹, Nils Gies^{4,5}, Thórdís Högnadóttir¹, Ásta Rut Hjartardóttir¹, Virginie Pinel⁶, Etienne Berthier⁷, Tobias Dürig¹, Hannah Iona Reynolds¹, Christopher W. Hamilton^{1,8}, Gumundur Valsson³, Páll Einarsson¹, Daniel Ben-Yehoshua⁹, Andri Gunnarsson¹⁰, Björn Oddsson¹¹

¹ Nordic Volcanological Center, Institute of Earth Sciences, University of Iceland, Sturlugata 7, 102 Reykjavík, Iceland.

² Institute of Earth Sciences, University of Iceland, Sturlugata 7, 102 Reykjavík, Iceland.

³ National Land Survey of Iceland, Stillholt 16–18, 300 Akranes.

⁴ Icelandic Institute of Natural History, Urriaholtsstræti 6–8, 210 Garabær, Iceland.

⁵ Institute of Geological Sciences, University of Bern, Baltzerstrasse 3, 3012 Bern, Switzerland.

⁶ Univ. Grenoble Alpes, Univ. Savoie Mont Blanc, CNRS, IRD, Univ. Gustave Eiffel, ISTerre, 38000 Grenoble, France.

⁷ LEGOS CNRS, University of Toulouse, 31400, Toulouse, France.

⁸ The University of Arizona, 1629 E University Blvd Tucson, AZ 85721-0092, USA.

⁹ Faculty of Civil and Environmental Engineering, University of Iceland, Dunhagi 5, 107 Reykjavík, Iceland.

¹⁰ The National Power Company of Iceland (Landsvirkjun), Háaleitisbraut 68, 103 Reykjavík, Iceland.

¹¹ The Department of Civil Protection and Emergency Management, Skógarhlí 14, 105 Reykjavík, Iceland.

Corresponding author: Gro B. M. Pedersen (gro@hi.is)

Key Points:

- Near real-time photogrammetric monitoring of the 2021 Fagradalsfjall eruption
- Acquisition of an unprecedented temporal data set including volume, effusion rate, orthomosaics, thickness maps and thickness change maps
- After six months of eruption the lava covers 4.8 km², with a bulk volume of $\sim 1.5 \times 10^8$ m³ and mean effusion rate of ~ 9.5 m³/s

Abstract

The basaltic effusive eruption at Mt. Fagradalsfjall began on March 19, 2021, ending a 781-year hiatus on Reykjanes Peninsula, Iceland. By late September 2021, 32 near real-time photogrammetric surveys were completed using satellite and airborne images, usually processed within 3–6 hours. The results provide unprecedented temporal data sets of lava volume, thickness, and effusion rate. This enabled rapid assessment of eruption evolution and hazards to populated areas, important infrastructure, and tourist centers. The mean lava thickness exceeds 30 m, covers 4.8 km² and has a bulk volume of $150 \pm 3 \times 10^6$ m³. The March–September mean effusion rate is 9.5 ± 0.2 m³/s, ranging between 1–8 m³/s in March–April and increasing to 9–13 m³/s in May–September. This is uncommon for recent Icelandic eruptions, where the highest discharge usually occurs in the opening phase.

Plain Summary

On March 19, 2021, an eruption began at Mt. Fagradalsfjall after 781-years dormancy on the Reykjanes Peninsula, Iceland. To monitor and evaluate hazards of the eruption, satellite and airborne stereoisimages were processed and made publicly available on the same day as they were surveyed. The data were used to create 3D models of the lava and update the lava volume and growth rate. The resulting maps were used by disaster response teams to evaluate the risk of the lava flow to nearby infrastructure and to manage tourism in the vicinity of the eruption. On September 30, 2021, the new lava flow-field covered 4.8 km², was up to 124 m thick and had a mean thickness of 30 m, yielding a total bulk volume of 150 million m³. The mean discharge during the six months of the eruption was 9.5 m³/s, equivalent to filling one Olympic swimming pool every four minutes.

Key Words:

Effusive eruption, lava flows, near real-time monitoring, Fagradalsfjall, photogrammetry

1. Introduction

Effusion rates and volumes of lava flows are key eruption parameters necessary for evaluation of hazards posed by basaltic eruptions. Various methods exist to monitor and quantify near-real time effusion rate ranging from localized channel and tube estimates of instantaneous effusion rate to time-averaged discharge rate (TADR) based on satellite-based thermal data and synthetic aperture radar data (see Harris et al., 2007, Poland, 2014 and references therein). Photogrammetric methods are more recurrently and effectively applied in monitoring effusive eruptions (e.g., Dietterich et al. 2021). This study presents a significant achievement in full-scale monitoring of a lava field with photogrammetric methods that yielded daily to weekly 3-D models and effective near real-time processing and presentation of results. We show how near real-time photogrammetric monitoring in the Fagradalsfjall 2021 eruption provided key information necessary for evaluating hazards and delivering data products to Civil Protection, local police, and the public.

On March 19, 2021, an eruption started at Mt. Fagradalsfjall ending a 781-year eruption hiatus on the Reykjanes Peninsula, Iceland (Fig. 1). Fagradalsfjall is a broad hyaloclastite tuya located within an oblique spreading zone, characterized by volcanic systems and strike-slip faults that are associated with the Mid-Atlantic plate boundary (e.g., Klein et al., 1977; Gee, 1998; Clifton and Kattenhorn, 2006; Einarsson et al., 2020, Sæmundsson et al., 2020). Eruptions in Reykjanes occur from eruptive fissures, that may focus onto a single vent to form lava shields. When occurring under a glacier, these eruption types form cones, tindars or tuyas (e.g., Jones, 1969, Pedersen and Grosse, 2014). At least in the last four thousand years, volcanic activity on the Reykjanes Peninsula has been episodic, with multiple eruptions occurring over several hundred years followed by ~ 800 –1000 years of quiescence. The last eruptive period ended in 1240 CE (Sæmundsson et al., 2020).

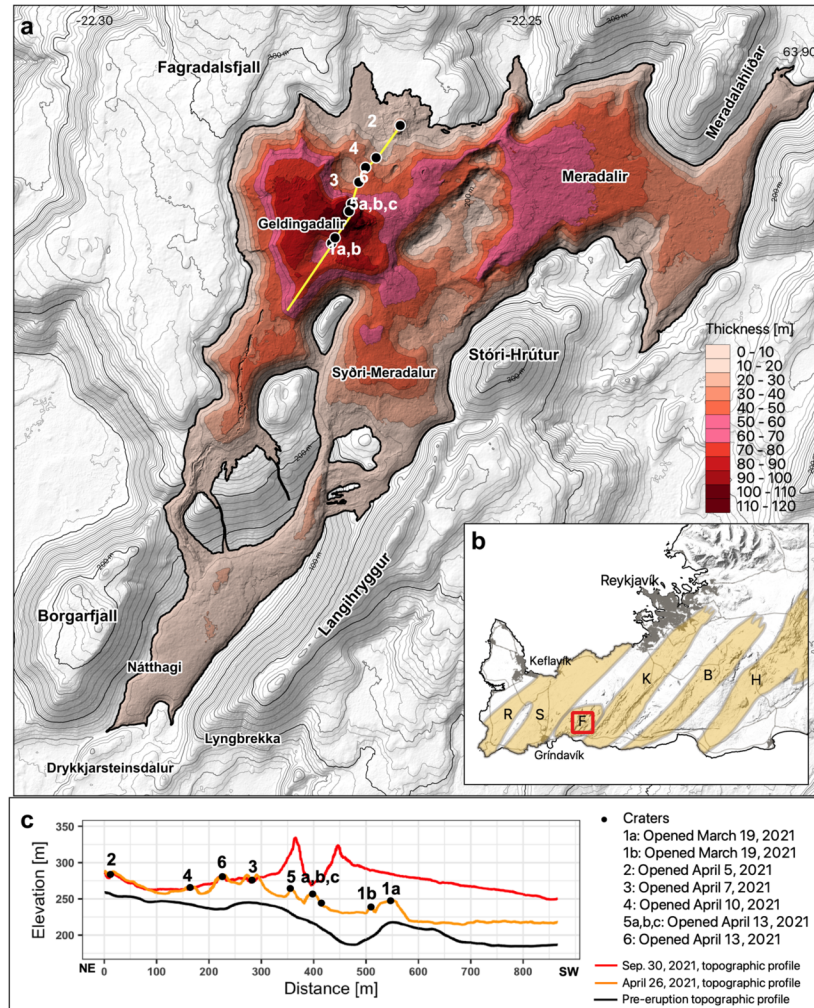


Figure 1 a) Thickness map of the erupted products in the Fagradalsfjall eruption by September 30, 2021. Vents are marked with a dot and numbered chronologically after opening time. Location of topographic profile in c) is marked as a yellow line. b) Map of the Reykjanes Peninsula. The red box indicates the area displayed in a). Densely populated areas are marked in gray. Volcanic systems (Sæmundsson and Sigurgeirsson, 2013) are marked with orange and denoted by capital letter according to their name; R: Reykjanes, S: Svartsengi, F: Fagradalsfjall, K: Krýsuvík, B: Brennisteinsfjöll, H: Hengill. c) Topographic profile along the vents from NE to SW (location see a).

2. Data and methods

The data used for near real-time monitoring of the Fagradalsfjall 2021 eruption consists mainly of aerial photographs and Pléiades stereoisimages and by September 30, 2021, 32 surveys had been carried out (Supplement S1, Table S1). The processing of the Pléiades stereoisimages is described in Gouhier et al. (submitted).

The airborne photogrammetric surveys of the eruption started on the morning of March 20, 2021, 11 hours after the eruption began. The bulk of surveys were done with the TF-BMW Partenavia P 68 Observer II survey aircraft operated by Garafug Corp (Table S1) with a Hasselblad A6D 100 MP medium-format camera with a 35 mm focal lens. Images were taken vertically at an altitude of 550–1800 m.a.s.l. with 75–90% overlap and image resolution of 7–30 cm. Up to 24 ground control points were placed around the lava flow-field and

measured with a high-precision GNSS instrument (see Supplement S1).

The aerial photographs were processed in the software MicMac (Pierrot Deseilligny et al., 2011, Rupnik et al., 2017), following the semi-automated workflow of Belart et al. (2019), as well as in Agisoft Metashape (version 1.7.3) and Pix4D mapper (version 4.6.4) yielding the DEMs and orthomosaics. Each DEM was compared with a pre-eruption DEM and with the previous survey done, obtaining a thickness map and a thickness change map (Fig. 2 and 3).

Lava outlines were manually digitized from the orthomosaics. Volumes were calculated using the mean thickness of the erupted deposit multiplied by its area. The uncertainties of the volume were obtained using the Normalized Mean Absolute Deviation (Höhle and Höhle, 2009) of the stable areas surrounding the lavas, as proxy for the uncertainties of the thickness maps. The uncertainties of the TADR are described in Supplement S1.

3. Results

After each survey the data products: DEMs (2×2 m), orthomosaics (0.2×0.2 m to 0.5×0.5 m), thickness maps (2×2 m), and lava outlines were completed and made available, usually 3–6 hours after acquisition. A low-resolution 3D model was also released to the public (<https://www.ni.is/midlun/utgafa/thrividdarlikon/eldgos-vid-fagradalsfjall>) within 1–3 hours for visualization purposes. Thanks to the short latency of data delivery the data products became important for the civil protection authorities. The orthomosaics and lava outlines were made available through an interactive map <http://atlas.lmi.is/mapview/?application=umbrotasja> and for geographic information systems through a Web Map Service (<https://gis.lmi.is/mapcache/reykjaneseldar/web-mercator/wms>). Figure S1 provides an example of data products delivered from each survey and table S2 provides results from each survey.

Here, we describe the evolution of the eruption, the erupted volume and TADR, as well as the lava flow-field development. Short-term fluctuations (minutes to hours) are not resolved by these measurements.

3.1. Fagradalsfjall eruption: Volume, discharge and lava field evolution

The eruption from March 19, 2021 to September 18, 2021 can be divided into five phases.

Phase 1 of the eruption (March 19 to April 5) began when a 180 m long fissure opened on March 19 around 20:30 in the Geldingadalir valley, which is located east of Mt. Fagradalsfjall (Fig. 1). Soon the eruption concentrated on two neighboring vents and the lava started infilling the valley (Fig. 2a). During this phase, the TADR ranged from 7.9 to $0.7 \text{ m}^3/\text{s}$ with a mean for the entire phase of $4.9 \pm 0.1 \text{ m}^3/\text{s}$ (Fig. 2b). The lava area increased to 0.33 km^2 , while the mean thickness increased to 22 m reaching a lava volume of $7.1 \times 10^6 \text{ m}^3$ before phase 2 started.

In phase 2 (April 5 to April 28) the active vent migrated (Fig. 1). Multiple eruption segments opened, starting on April 5, when two new fissure-segments opened 800 m northeast of the first fissure segments. Another fissure opened at midnight on April 7, another one on April 10 at and then again on April 13 when two new fissure segments opened. Each fissure segment concentrated into 1–2 circular vents, which over the following 10 days became inactive, except for southern the vents that developed from the April 13 fissure segments. Phase 2 had similar TADR as in phase 1 in the range $4.6\text{--}7.5 \text{ m}^3/\text{s}$ with the highest TADR observed just after new vent openings. The mean TADR in this period was $6.3 \pm 0.4 \text{ m}^3/\text{s}$ and the volume increased to $19.4 \times 10^6 \text{ m}^3$. With the migration of active vent locations, lava started to flow into the valleys of Meradalir (April 5), Geldingadalir and Syri-Meradalur (April 14) covering an area of 1.1 km^2 with a mean thickness of 16 m.

In phase 3 (April 28 to June 28) the vent activity stabilized at one location. Most of the time (May 2 to June 12) it exhibited cycles of short-term (ca. 8–9 minutes) pulsations. The TADR increased from 8.8 to a maximum of $13.0 \text{ m}^3/\text{s}$ with a phase mean of $11.4 \pm 0.5 \text{ m}^3/\text{s}$. The “fill and spill” from one valley into another increased the area stepwise to 3.82 km^2 with mean thickness of 20.8 m yielding a volume of $79.8 \times 10^6 \text{ m}^3$.

The lava migrated to Nátthagi valley through Syri-Meradalir (May 22) and through southern Geldingadalir (June 13).

Phase 4 (June 28 to September 2) was characterized by episodic activity with intense lava emplacement (ca. 12–24 hours) followed by inactive periods of similar length. Despite the episodic activity this period had only slightly lower TADR to phase 3 with a mean TADR for the whole phase of $11.0 \pm 0.4 \text{ m}^3/\text{s}$ ranging from 8.5 to $11.1 \text{ m}^3/\text{s}$ and the volume increased to $142.5 \times 10^6 \text{ m}^3$. The lava thickened to around 50 m northeast of the active crater due to episodic overflows and in Meradalir the lava thickened by $\sim 25 \text{ m}$ due to stacking and inflation.

The eruption's rhythm changed again in the phase 5 (September 2 to 18), when a week-long pause from September 2–11, was followed by week-long period of activity from September 11–18. The measured TADR was $12.2 \text{ m}^3/\text{s}$ for September 9–17. The mean TADR for phase 5 is $5.6 \pm 0.6 \text{ m}^3/\text{s}$ and the volume increased to $150.8 \times 10^6 \text{ m}^3$. Most of the deposition was in Geldingadalir, where a 10–15 m thick lava pond was established north-northwest of the active crater between September 11 to 15, that partly drained through an upwelling zone towards south and into Nátthagi from September 15 to 18. At the time of writing (November 18), no eruptive activity has been observed since September 18.

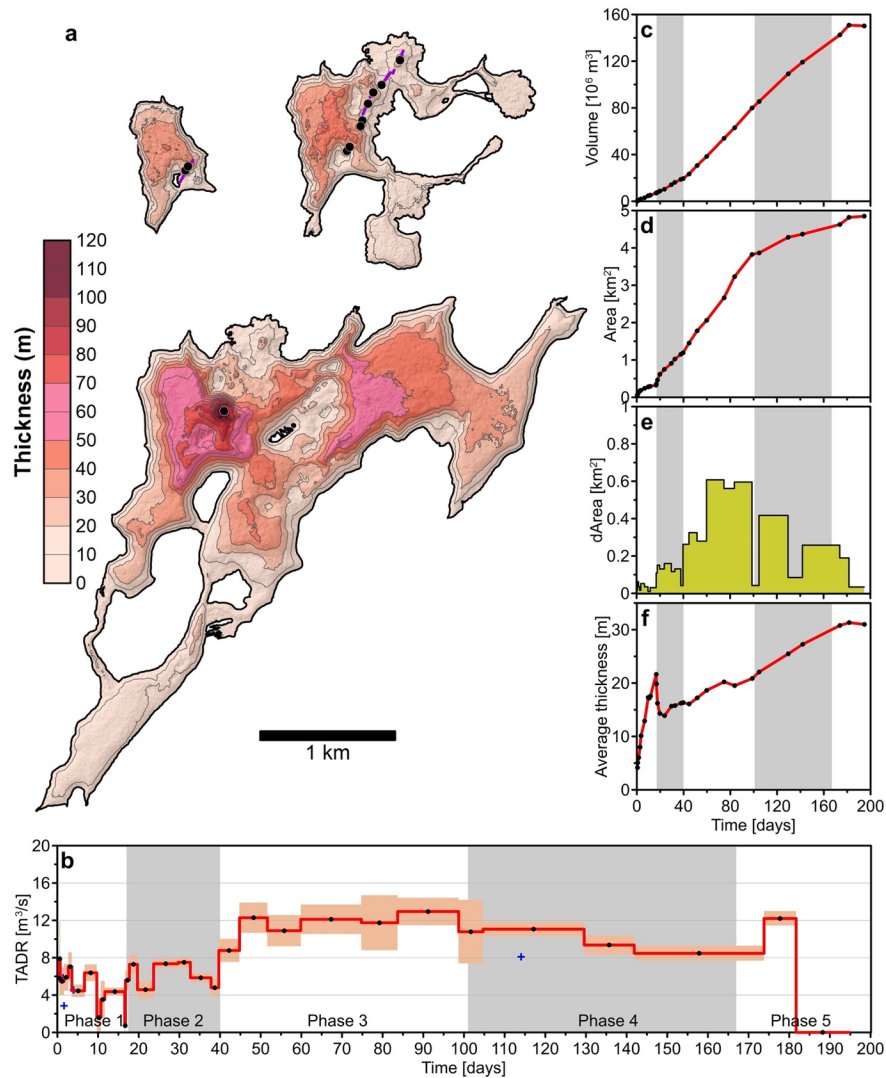


Figure 2 a) The thickness of erupted material by the end of phase 1 (April 5), end of phase 2 (April 26) and phase 4 (August 8, 2021). Purple line denotes initial fissure segment b–f) Eruption parameters of the Fagradalsfjall 2021 eruption showing the evolution of time-average discharge rate (TADR), volume, area, area change (dArea), and mean thickness. Orange boxes denote uncertainty in measurement. Blue crosses denote supporting TADR measurements (Supplement S2).

3.2. Lava transport systems and emplacement

Processes related to lava transport and emplacement could be studied through thickness change maps (Fig. 3a–c) such as breakouts, inflation, lava stacking, pond formation, channel changes, deflation, cooling and contraction as well as vent changes. Especially, monitoring of inflation within valleys that were likely to spill into lower lying terrain was important since some sections of popular hiking trails were located below lava-filled valleys.

Despite the relatively stable effusion rate in phase 3 and 4 (Fig. 2), the braided lava pathways and the lava advancement were complex and variable as the lava filled and spilled from one valley into another. Short-term prediction of the timing of overflow from one valley to another provided challenges and thus monitoring the changes in the lava transport system and lava deposition in different valleys became important. The lava pathways were strongly controlled by the topography and mainly confined to the valleys and the steep slopes connecting them. However, since the valley systems consisted of multiple valleys east and south of the active vents the lava pathways were not uniformly filling up the valleys but switching from one valley to another. One way to monitor these changes and estimate the variability was to investigate the volume changes in different zones and vent distances (at 100 m interval) based on the thickness change maps. For each zone we could calculate the $\Delta V/\Delta t$ reflecting the volume deposited for a given period at a specific vent distance. This allows us to display the changes in lava transport and deposition in between these zones and distances over time (Fig. 3d).

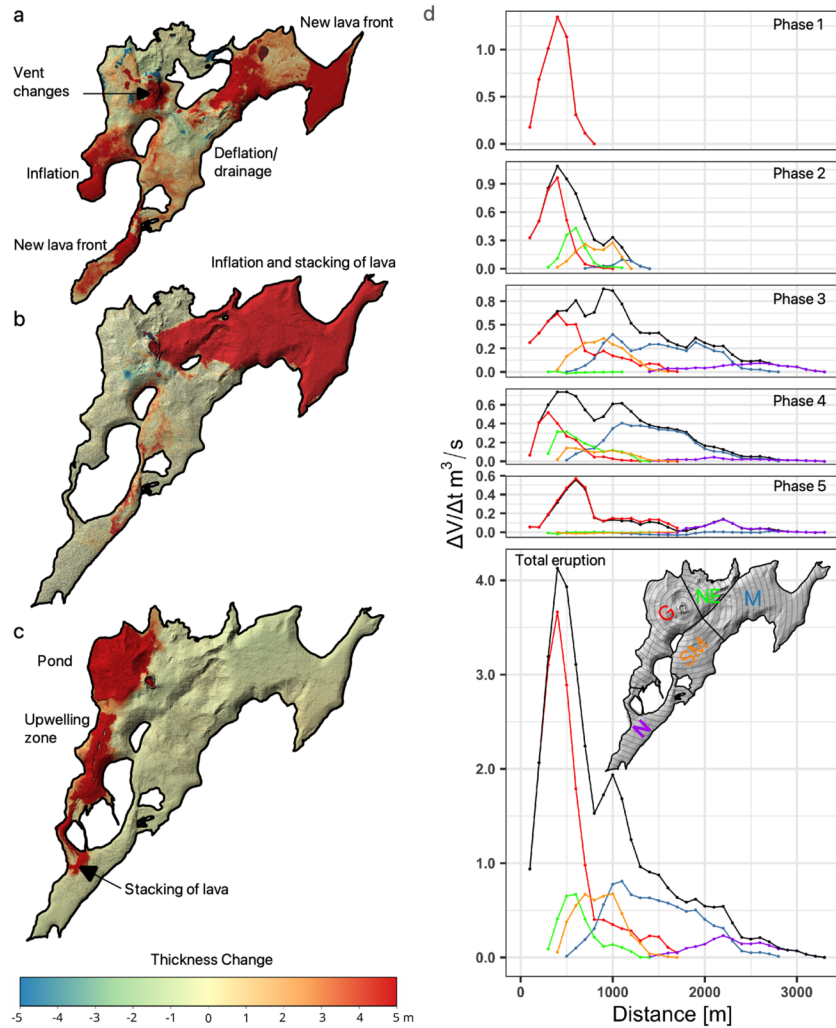


Figure 3 Thickness change map from a) June 2–11 b) July 2–27 and c) September 9–17 showing observable emplacement processes. d) $\Delta V/\Delta t$ as a function of vent distance for each phase in five zones (see inset for location); G: Geldingadalir, M: Meradalir, SM: Syri-Meradalur, N: Nátthagi and NE: the plateau northeast of the vent. The black line is the total $\Delta V/\Delta t$ for all five zones as a function of vent distance. In phase 1 all lava was deposited in Geldingadalir and thus the total $\Delta V/\Delta t$ is equal to the $\Delta V/\Delta t$ for Geldingadalir. The lower panel shows the total deposition from March to September between zones as a function of vent distance.

The lava deposition as a function of vent distance changed markedly over time. In phase 1 all lava was emplaced within Geldingadalir; and, in phase 2, as new vents opened on the northeast plateau, lava migrated into Meradalir and Syri-Meradalur. In phase 3, the lava field expanded to its current maximum extent, reaching 3.3 km from the vent by having lava ponds acting as reservoirs for the transport system (Fig. 3d). This lava transport system closed during phase 4, when the continuous lava effusion was replaced by episodic activity responsible for large overflows and significant stacking in the vent region. Stacking and inflation was continued in Meradalir, where the lava reached a distance of 2.8 km from the vent. Thus, despite the long-term TADR in phases 3 and 4 was similar (Fig. 2), the difference between continuous and

episodic activity at the vent had a major impact on the lava transport system and the ability of the lava field to expand. In phase 5, most lava emplacement was within a 1 km radius of the active vent but reached 2.7 km in mid-September after the drainage of a pond northwest of the crater (Fig. 3c). Between surveys this variation of lava deposition between zones amounted to as much as 10 m³/s for Geldingadalir and Meradalir, 5 m³/s for Syri-Meradalur and the Northeast plateau and 3 m³/s for Nátthagi. Thus, despite a stable TADR, the local effusion into individual valleys varied significantly between surveys providing a great challenge for forecasting the timing of lava spilling from one valley to another.

4. Discussion

Satellite and airborne photogrammetry provided flexible methods for near real-time monitoring of volume and TADR on a daily to weekly basis for Icelandic conditions, where low vegetation and very changeable weather prevails. Airplane surveys were possible for cloud cover down to 550 m.a.s.l and could be deployed quickly since the flight to the eruption only takes 10 minutes from Reykjavík Airport (RVK). The acquisitions were mainly limited by the low cloud, and occasionally by lack of available aircraft.

The data products (orthomosaics, DEM, lava outline, thickness maps, thickness change maps and volume and TADR estimates) provided critical information for disaster response and for the scientific community. The volume and TADR were used to evaluate the status of the eruption and as input parameters together with the thickness maps for lava flow simulation. The orthomosaics and lava outlines were important to responders providing base maps for infrastructure, planning, rescue missions, and for tourists visiting the eruption.

The effusion rate evolution for basaltic eruptions provides important insights to increase understanding of the source of the magma and the conduit properties. Different trends in effusion rate evolution have been classified into types and linked to specific plumbing system dynamics (Harris et al., 2000, 2011, Araveno et al., 2020). Type I is characterized by a phase of high initial effusion followed by an extended phase of waning effusion, which has been interpreted as a tapping of a pressurized reservoir (Wadge et al., 1981) and efficient magma ascent in early stages (Araveno et al., 2020). Type II has a low, near-constant effusion rate and has been related to low values of overpressure (5–10 MPa), consistent with overflow in a non-pressurized system (Harris et al. 2000, Araveno et al., 2020). In type III eruptions, the effusion rate increases with time and has been suggested to be linked with ascent of a magma batch, pushing a volume of degassed magma ahead (Harris et al., 2011). However, this trend has also been linked to conduit erosion caused by high erosion coefficients, high initial overpressures, and/or large magma reservoirs, that in its extreme case may lead to a sudden overpressure drop and eruption shutdown caused by high effusion rate and magma withdrawal (Araveno et al., 2020). The last type is type IV, which shows highly pulsating effusion rate and has been related to ascent of multiple batches of magma (Harris et al., 2011).

The Fagradalsfjall 2021 eruption started with low and stable effusion rate between 4–8 m³/s in phase 1–2 (Fig. 2) and initially had the characteristics of a type II eruption. However, in phase 3–4 the effusion rate increased to 8–13 m³/s changing the characteristics to resemble a type III eruption, whilst in phase 5 the TADR had pulsating characteristics similar to type IV but lasted only for a month. The low initial effusion rate at Fagradalsfjall is between 30 and 2500 times smaller than other recorded Icelandic eruptions in the last 75 years (Gudmundsson et al., 2004, 2012, Jude-Eton et al., 2012, Hreinsdóttir et al., 2014, Pedersen et al., 2017, 2018, Thorarinsson, 1964, 1967). When normalizing the initial effusion rate to the mean output rate (Harris et al. 2007) of each eruption, it becomes clear that it is not only a low initial effusion rate that is unusual, but the evolution of the effusion rate at Fagradalsfjall, which is unlike any observations from previous recent Icelandic eruptions (Fig. 4).

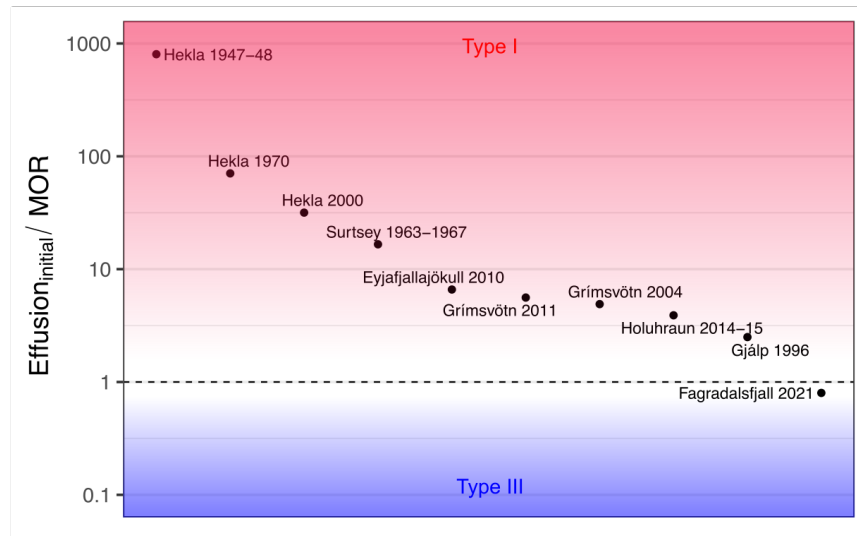


Figure 4 Fagradalsfjall effusion characteristics described by the ratio of initial effusion rate $\text{Effusion}_{\text{initial}}$ divided by the Mean Output Rate, MOR (Harris et al., 2007) compared to other recent Icelandic eruptions (Gudmundsson et al., 2004, 2012, Jude-Eton et al., 2012, Hreinsdóttir et al., 2014, Pedersen et al., 2017, 2018, Thorarinnsson, 1964, 1967). Note the y-axis is logarithmic. Fagradalsfjall 2021 is clearly an outlier with a ratio below 1, while all other eruptions plot above 1. The effusion rate evolution of types I and III from Harris et al (2000, 2011) has been indicated in red and blue. Type II should ideally plot along the dashed line, while the pulsating nature of type IV could plot everywhere in the plot.

For the first time we observe an eruption that primarily has characteristics of a type III eruption, while recent Icelandic eruptions show characteristics that resemble type I eruptions. Based on the interpretation of type I eruptions, it makes sense that eruptions in Hekla, Grímsvötn and Bárarbunga (Holuhraun 2014–2015) all show effusion rate evolution controlled by pressurized reservoirs, since these volcanic systems show evidence of having magma chambers (e.g., Ofeigsson et al., 2011, Geirsson et al., 2012, Hreinsdóttir et al., 2014, Gudmundsson et al., 2016). Less information exists for the Vestmannaeyjar volcanic system responsible for the Surtsey 1963–1967 eruption, but based on the available data (Thorarinnsson, 1964), the effusion rate evolution suggests that Fagradalsfjall is unlike this eruption as well.

The evolution of the effusion rate of type III eruptions has been linked to the ascent of a single magma batch, pushing a volume of degassed magma ahead (Harris et al., 2011, Steffke et al., 2011). Interestingly, geochemical evidence suggests that in phase 1–2 the magma plumbing system gradually changed from being fed from a depleted shallow mantle source to being fed by more enriched discrete melts from greater depth (Marshall et al., 2021). Nevertheless, this gradual geochemical change happened during the first 40 days of the eruption, where the TADR is stable and the increase in TADR happen around day 50. However, during phase 2, new vents opened at locations which were 60 m above the initial vents in Geldingadalir (Fig. 1) suggesting an increase in pressure during this time (in the order of 1–1.5 MPa based on higher lithostatic load corresponding to 60 m increase in elevation of vents). By the end of phase 2, the vents at the higher elevations had shut off and the effusion from vent 5, which is located in similar elevation as vent 1a,b increased from 7 to 13 m^3/s in phase 3, while displaying fire fountain activity.

The delay between the geochemical change and the increased effusion is intriguing. In the 2018 Kilauea eruption the increase in effusion started within a day of an observed change to more mafic magma increasing the effusion from 6.5 m^3/s to 110 m^3/s (Gansecki et al., 2019, Dietterich et al., 2021). Furthermore, this

change was associated with observed deformation and earthquake activity. Thus, there was a clear link between a change in geochemistry and a substantial increase in effusion.

If the effusion increase in Fagradalsfjall is related to ascent of a magma batch pushing a degassed magma ahead (which would be $20 \times 10^6 \text{ m}^3$ based on the erupted bulk volume estimates at day 40), then it is clear that it is a more subtle process compared to the 2018 Kīlauea eruption, potentially involving lower overpressure and slower increase in effusion.

Another possible model used to explain increase in effusion with thermal erosion. The eruption in phase 1–2 displayed type II characteristics consistent with overflow in a non-pressurized system. The effusion rate and the successive vent openings suggest that the system was not highly pressurized. Over time the heating of the conduit walls enabled sufficient thermal erosion to increase the effusion rate, which for a cylindrical conduit is proportional to r^4 , where r is radius (e.g., Turcotte and Schubert, 2002). This process may have been enhanced by the increased temperature of the magma due to an increase in MgO from 8.8–9.7% (Marshall et al., 2021). We consider this conduit-controlled flow a plausible model for Fagradalsfjall because it explains the sharp contrast with the behavior to other Icelandic eruptions (e.g., Hekla, Grímsvötn and Bárarbunga) where pressure in a magma chamber is considered the main control of flow (e.g., Hreinsdóttir et al., 2014).

5. Conclusions

Near real-time photogrammetric monitoring of the eruption at Fagradalsfjall 2021 was performed using a combination of satellite and airborne stereomages as a part of the response to the event. This provided essential eruption parameters such as volume and effusion rate, as well as the maps distributed to the public, the Civil Protection, rescue teams, and the tourism industry.

By September 30, 2021, 32 surveys have been performed. Currently, the lava flow-field covers 4.8 km^2 and the estimated bulk volume (including vesicles and macroscale porosity) is $150 \times 10^6 \text{ m}^3$, yielding a mean effusion rate (from the beginning of the eruption start) of $9.5 \pm 0.2 \text{ m}^3/\text{s}$.

The lava pathways and lava advancement were very complex and changeable as the lava filled and spilled from one valley into another and short-term prediction of the timing of overflow from one valley to another proved challenging. Analysis of thickness maps and thickness change maps show that the lava transport into different valleys varied up to $10 \text{ m}^3/\text{s}$ between surveys as lava transport rapidly switched between one valley to another.

Compared to recent Icelandic eruptions, the evolution of the effusion rate is very unusual, having a very low and stable effusion in phase 1–2 and increasing effusion in phase 3. This behavior may be due to widening of the conduit by thermal erosion with time, and not controlled by magma chamber pressure as is most common in the volcanic zones of Iceland.

Acknowledgements

The data from airborne surveys will be available on <https://zenodo.org/> and data from Pléiades will be available on <https://www.theia-land.fr/en/product/pleiades/>. The processed data is currently available in the Supporting Information for the purposes of review.

We would like to thank our pilots Ú. Henningsson, K. Kárason, K. Halldórsdóttir, G. Árnason, J.Sverrisson, the Icelandic Coast Guard and Iceland Aviation Service for their commitment to carry out flights. The authors would like to acknowledge the Icelandic Research fund, Grant No. 206755-052, the Fulbright–NSF Arctic Scholar program, NSF RAPID program and the French Space Agency (CNES) for their support. Pléiades images were provided under the CREST² (CNES) initiative during the first 10 days of the eruption and through the Icelandic Volcanoes Supersite project supported by the Committee on Earth Observing Satellites (image Pléiades©CNES2021, distribution AIRBUS DS).

References

Aravena, A., Cioni, R., Coppola, D., Vitturi, M. de' M., Neri, A., Pistolesi, M., & Ripepe, M. (2020). Effusion

Rate Evolution During Small-Volume Basaltic Eruptions: Insights From Numerical Modeling. *Journal of Geophysical Research: Solid Earth*, 125 (6), e2019JB019301. <https://doi.org/10.1029/2019JB019301>

Belart, J. M. C., Magnússon, E., Berthier, E., Pálsson, F., Aalgeirsdóttir, G., and Jóhannesson, T. (2019). The geodetic mass balance of Eyjafjallajökull ice cap for 1945-2014: processing guidelines and relation to climate. *J. Glaciol.* 65, 395–409. doi: 10.1017/jog.2019.16

Clifton, A. E., & Kattenhorn, S. A. (2006). Structural architecture of a highly oblique divergent plate boundary segment. *Tectonophysics*, 419 (1), 27–40. <https://doi.org/10.1016/j.tecto.2006.03.016>

Dietterich, H. R., Diefenbach, A. K., Soule, S. A., Zoeller, M. H., Patrick, M. P., Major, J. J., & Lundgren, P. R. (2021). Lava effusion rate evolution and erupted volume during the 2018 Kīlauea lower East Rift Zone eruption. *Bulletin of Volcanology*, 83(4), 25. <https://doi.org/10.1007/s00445-021-01443-6>

Einarsson, P., Hjartardóttir, Á. R., Imsland, P., Hreinsdóttir, S. (2020). The structure of seismogenic strike-slip faults in the eastern part of the Reykjanes Peninsula oblique rift, SW Iceland. *Journal of Volcanology and Geothermal Research* 106372, doi:10.1016/j.jvolgeores.2018.04.029.

Gansecki, C., Lee, R. L., Shea, T., Lundblad, S. P., Hon, K., & Parcheta, C. (2019). The tangled tale of Kīlauea’s 2018 eruption as told by geochemical monitoring. *Science*, 366 (6470). <https://doi.org/10.1126/science.aaz0147>

Gardelle J., Berthier E., Arnaud Y. & Kääb, A. (2013) Region-wide glacier mass balances over the Pamir - Karakoram - Himalaya during 1999-2011. *The Cryosphere*, 7, 1263-1286, doi: 10.5194/tc-7-1263-2013.

Gee, M. A. M. (1998). *Volcanology and geochemistry of Reykjanes Peninsula: Plume-mid-ocean ridge interaction*. [PhD]. University of London.

Geirsson, H., LaFemina, P., Árnadóttir, T., Sturkell, E., Sigmundsson, F., Travis, M., Schmidt, P., Lund, B., Hreinsdóttir, S., & Bennett, R. (2012). Volcano deformation at active plate boundaries: Deep magma accumulation at Hekla volcano and plate boundary deformation in south Iceland. *Journal of Geophysical Research: Solid Earth*, 117(B11). <https://doi.org/10.1029/2012JB009400>

Gouhier, M., Pinel, V., Belart, J. DeMichele, M. Proy, C., Tinel, C., Berthier, E., Guéhenneux, Y., Gudmundsson, M. T., Óskarsson B. V., Gremion, S., Raucoules, D., Valade, S., Massimetti, F. Oddsson, B. (submitted). CNES-ESA satellite contribution to the operational monitoring of volcanic activity: The 2021 Icelandic eruption of Mt. Fagradalsfjall. *Journal of Applied Volcanology*

Gudmundsson, M.T., Högnadóttir, ., Kristinsson, A.B., Gudbjörnsson, S. (2007). Geothermal activity in the subglacial Katla caldera, Iceland, 1999-2005, studied with radar altimetry. *Annals of Glaciology*, 45, 66-72, doi.org/10.3189/172756407782282444.

Gudmundsson, M.T., K. Jónsdóttir, A. Hooper, E.P. Holohan, S.A. Halldórsson, B.G. Ófeigsson, S. Cesca, K.S. Vogfjörð, F. Sigmundsson, Th. Högnadóttir, P. Einarsson, O. Sigmarsson, A.H. Jarosch, K. Jónasson, E. Magnússon, S. Hreinsdóttir, M. Bagnardi, M.M. Parks, V. Hjörleifsdóttir, F. Pálsson, T.R. Walter, M.P.J. Schöpfer, S. Heimann, H.I. Reynolds, S. Dumont, E. Bali, G.H. Gudfinnsson, T. Dahm, M.J. Roberts, M. Hensch, J. M.C. Belart, K. Spaans, S. Jakobsson, G.B. Gudmundsson, H.M. Fridriksdóttir, V. Drouin, T. Dürig, G. Adalgeirsdóttir, M.S. Riishuus, G.B.M. Pedersen, T. van Boeckel. B. Oddsson, M.A. Pfeffer, S. Barsotti, B. Bergsson, A. Donovan, M.R. Burton, A. Aiuppa. (2016). Gradual caldera collapse at Bárðarbunga volcano, Iceland regulated by lateral magma outflow. *Science* 353, aaf8988. DOI: 10.1126/science.aaf8988.

Gudmundsson, M. T., Sigmundsson, F., Björnsson, H., & Högnadóttir, T. (2004). The 1996 eruption at Gjalp, Vatnajökull ice cap, Iceland: Efficiency of heat transfer, ice deformation and subglacial water pressure. *Bulletin of Volcanology*, 66 (1), 46–65. <https://doi.org/10.1007/s00445-003-0295-9>

Gudmundsson, M.T., Thordarson, T., Höskuldsson, Á., Larsen G., Björnsson, H., Prata, A.J., Oddsson, B., Magnússon, E., Högnadóttir, T., Pedersen, G.N., Hayward, C.L., Stevenson, J.A., Jónsdóttir, I. (2012). Ash

generation and distribution from the April-May 2010 eruption of Eyjafjallajökull, Iceland. *Scientific Reports* , 2, 572; DOI:10.1038/srep00572

Harris, A. J. L., Dehn, J., & Calvari, S. (2007). Lava effusion rate definition and measurement: A review. *Bulletin of Volcanology* , 70 (1), 1. <https://doi.org/10.1007/s00445-007-0120-y>

Harris, A. J. L., Murray, J. B., Aries, S. E., Davies, M. A., Flynn, L. P., Wooster, M. J., Wright, R., & Rothery, D. A. (2000). Effusion rate trends at Etna and Krafla and their implications for eruptive mechanisms. *Journal of Volcanology and Geothermal Research* , 102 (3), 237–269. [https://doi.org/10.1016/S0377-0273\(00\)00190-6](https://doi.org/10.1016/S0377-0273(00)00190-6)

Harris, A., Steffke, A., Calvari, S., & Spampinato, L. (2011). Thirty years of satellite-derived lava discharge rates at Etna: Implications for steady volumetric output. *Journal of Geophysical Research: Solid Earth* , 116 (B8). <https://doi.org/10.1029/2011JB008237>

Hreinsdóttir, S., Sigmundsson, F., Roberts, M. J., Björnsson, H., Grapenthin, R., Arason, Th., Árnadóttir, T., Hólmjárn, J., Geirsson, H., Bennett, R. A., Gudmundsson, M. T., Oddsson, B., Ófeigsson, B. G., Villemin, T., Jónsson, T., Sturkell, E., Höskuldsson, A., Larsen, G., Thordarson, T., & Óladóttir, B. A. (2014). Volcanic plume height correlated with magma-pressure change at Grímsvötn Volcano, Iceland. *Nature Geoscience* , 7 , 214–218. <https://doi.org/10.1038/ngeo2044>

Höhle, J. and Höhle, M. (2009). Accuracy assessment of digital elevation models by means of robust statistical methods, *ISPRS J. Photogramm. Remote Sens.* , 64, 398–406, doi:10.1016/j.isprsjprs.2009.02.003.

Jones, J. G. (1969). Intraglacial volcanoes of the Laugarvatn region, south-west Iceland—I. *Quarterly Journal of the Geological Society*, 124(1–4), 197–211. <https://doi.org/10.1144/gsjgs.124.1.0197>

Jude-Eton, T.C., Thordarson, Th., Gudmundsson, M.T., Oddsson, B. (2012). Dynamics, stratigraphy and proximal dispersal of supraglacial tephra during the ice-confined 2004 eruption at Grímsvötn volcano, Iceland. *Bull. Volc.* , 74, 1057–1082. DOI: 10.1007/s00445-012-0583-3.

Klein, F. W., Einarsson, P., & Wyss, M. (1977). The Reykjanes Peninsula, Iceland, earthquake swarm of September 1972 and its tectonic significance. *Journal of Geophysical Research (1896-1977)* , 82 (5), 865–888. <https://doi.org/10.1029/JB082i005p00865>

Marshall, E. W., Rasmussen, M. B., Halldorsson, S. A., Matthews, S., Ranta, E., Sigmarsson, O., Robin, J. G., Bali, E. , Caracciolo, A., Gudfinnsson, G. H. and Mibei, G. K. (2021) Rapid geochemical evolution of the mantle-sourced Fagradalsfjall eruption, Iceland. AGU Fall meeting, New Orleans, USA

Nuth, C. and Kääb, A. (2011). Co-registration and bias corrections of satellite elevation data sets for quantifying glacier thickness change. *The Cryosphere* , 5, 271–290, <https://doi.org/10.5194/tc-5-271-2011>.

Ofeigsson, B. G., Hooper, A., Sigmundsson, F., Sturkell, E., & Grapenthin, R. (2011). Deep magma storage at Hekla volcano, Iceland, revealed by InSAR time series analysis. *Journal of Geophysical Research: Solid Earth*, 116(B5). <https://doi.org/10.1029/2010JB007576>

Óskarsson, B. V.; Jónasson, K.; Valsson, G. & Belart, J. M. C. (2020). Erosion and sedimentation in Surtsey island quantified from new DEMs, *Surtsey Research*, 14, 63–77.

Pedersen, G. B. M., Belart, J. M. C., Magnússon, E., Vilmundardóttir, O. K., Kizel, F., Sigurmundsson, F. S., Gísladóttir, G., & Benediktsson, J. A. (2018). Hekla Volcano, Iceland, in the 20th Century: Lava Volumes, Production Rates, and Effusion Rates. *Geophysical Research Letters* , 45 (4), 1805–1813. <https://doi.org/10.1002/2017GL076887>

Pedersen, G. B. M., & Grosse, P. (2014). Morphometry of subaerial shield volcanoes and glaciovolcanoes from Reykjanes Peninsula, Iceland: Effects of eruption environment. *Journal of Volcanology and Geothermal Research* , 282 , 115–133. <https://doi.org/10.1016/j.jvolgeores.2014.06.008>

Pedersen, G. B. M., Höskuldsson, A., Dürig, T., Thordarson, T., Jónsdóttir, I., Riishuus, M. S., Óskarsson, B. V., Dumont, S., Magnússon, E., Gudmundsson, M. T., Sigmundsson, F., Drouin, V. J. P. B., Gallagher, C.,

Askew, R., Gudnason, J., Moreland, W. M., Nikkola, P., Reynolds, H. I., & Schmith, J. (2017). Lava field evolution and emplacement dynamics of the 2014–2015 basaltic fissure eruption at Holuhraun, Iceland. *Journal of Volcanology and Geothermal Research* , 340 , 155–169. <https://doi.org/10.1016/j.jvolgeores.2017.02.027>

Pierrot Deseilligny, M., and Clery, I. (2011). Apero, an open source bundle adjustment software for automatic calibration and orientation of set of images. *Int. Arch. Photogr. Remote Sens. Spat. Inform. Sci.* 3816, 269–276. doi: 10.5194/isprsarchives-XXXVIII-5-W16-269-2011

Poland, M. P. (2014). Time-averaged discharge rate of subaerial lava at Kīlauea Volcano, Hawai‘i, measured from TanDEM-X interferometry: Implications for magma supply and storage during 2011–2013. *Journal of Geophysical Research: Solid Earth* , 119 (7), 5464–5481. <https://doi.org/10.1002/2014JB011132>

Porter, C., Morin, P., Howat, I., Noh, M.-J., Bates, B., Peterman, K., et al. (2018). *ArcticDEM* . Harvard Dataverse, V1. Polar Geospatial Center, University of Minnesota. doi: 10.7910/DVN/OHHUKH

Rupnik, E., Daakir, M., and Pierrot Deseilligny, M. (2017). MicMac - a free, open-source solution for photogrammetry. *Open Geospatial Data Softw. Stand.* 2:14. doi: 10.1186/s40965-017-0027-2

Sæmundsson, K., & Sigurgeirsson, M. Á. (2013). Reykjanesskagi. In J. Sólnes, F. Sigmundsson, & B. Bessason (Eds.), *Náttúruvá* (pp. 379–401). Vilagatrygging Íslands / Háskólaútgáfa.

Sæmundsson, K., Sigurgeirsson, M. Á., & Frileifsson, G. Ó. (2020). Geology and structure of the Reykjanes volcanic system, Iceland. *Journal of Volcanology and Geothermal Research* , 391 , 106501. <https://doi.org/10.1016/j.jvolgeores.2018.11.022>

Shean, D. E., Alexandrov, O., Moratto, Z. M., Smith, B. E., Joughin, I. R., Porter, C., Morin, P. (2016). An automated, open-source pipeline for mass production of digital elevation models (DEMs) from very-high resolution commercial stereo satellite imagery, *ISPRS Journal of Photogrammetry and Remote Sensing*, Vol. 116, pp 101-117, <https://doi.org/10.1016/j.isprsjprs.2016.03.012>.

Steffke, A. M., Harris, A. J. L., Burton, M., Caltabiano, T., & Salerno, G. G. (2011). Coupled use of COSPEC and satellite measurements to define the volumetric balance during effusive eruptions at Mt. Etna, Italy. *Journal of Volcanology and Geothermal Research* ,205 (1), 47–53. <https://doi.org/10.1016/j.jvolgeores.2010.06.004>

Sørensen, E. V. & Dueholm, M. (2018). Analytical procedures for 3D mapping at the Photogeological Laboratory of the Geological Survey of Denmark and Greenland, Geological Survey of Denmark and Greenland Bulletin, 41, 99-104. DOI:<https://doi.org/10.34194/geusb.v41.4353>.

Thorarinsson, S., Einarsson T, Sigvaldason G, Elisson G (1964) The submarine eruption off the Vestmann islands 1963-64 - A preliminary report. *Bulletin Volcanologique* 27:435–445. <https://doi.org/10.1007/BF02597544>

Thorarinsson, S. (1968) Heklueldar (In Icelandic: the Hekla fires).. Sögufélag. 185 pp.

Turcotte, D.L., Schubert, G. 2002. *Geodynamics*, 2nd Ed. Cambridge, University Press. 456 pp.

Wadge, G. (1981). The variation of magma discharge during basaltic eruptions. *Journal of Volcanology and Geothermal Research* ,11 (2), 139–168. [https://doi.org/10.1016/0377-0273\(81\)90020-2](https://doi.org/10.1016/0377-0273(81)90020-2)

Hosted file

agusupporting-information_2021119.docx available at <https://authorea.com/users/552161/articles/604655-volume-effusion-rate-and-lava-transport-during-the-2021-fagradalsfjall-eruption-results-from-near-real-time-photogrammetric-monitoring>

Volume, effusion rate, and lava transport during the 2021 Fagradalsfjall eruption:
Results from near real-time photogrammetric monitoring

Gro B. M. Pedersen^{1*}, Joaquin M. C. Belart^{2,3}, Birgir Vilhelm Óskarsson⁴,
Magnús Tumi Gudmundsson¹, Nils Gies^{4,5}, Thórdís Högnadóttir¹, Ásta Rut
Hjartardóttir¹, Virginie Pinel⁶, Etienne Berthier⁷, Tobias Dürig¹, Hannah Iona
Reynolds¹, Christopher W. Hamilton^{1,8}, Guðmundur Valsson³, Páll Einarsson¹,
Daniel Ben-Yehosua⁹, Andri Gunnarsson¹⁰, Björn Oddsson¹¹

¹ Nordic Volcanological Center, Institute of Earth Sciences, University of Iceland, Sturlugata 7, 102 Reykjavík, Iceland.

² Institute of Earth Sciences, University of Iceland, Sturlugata 7, 102 Reykjavík, Iceland.

³ National Land Survey of Iceland, Stillholt 16–18, 300 Akranes.

⁴ Icelandic Institute of Natural History, Urriðaholtsstræti 6–8, 210 Garðabær, Iceland.

⁵ Institute of Geological Sciences, University of Bern, Baltzerstrasse 3, 3012 Bern, Switzerland.

⁶ Univ. Grenoble Alpes, Univ. Savoie Mont Blanc, CNRS, IRD, Univ. Gustave Eiffel, ISTERre, 38000 Grenoble, France.

⁷ LEGOS CNRS, University of Toulouse, 31400, Toulouse, France.

⁸ The University of Arizona, 1629 E University Blvd Tucson, AZ 85721-0092, USA.

⁹ Faculty of Civil and Environmental Engineering, University of Iceland, Dunhagi 5, 107 Reykjavík, Iceland.

¹⁰ The National Power Company of Iceland (Landsvirkjun), Háaleitisbraut 68, 103 Reykjavík, Iceland.

¹¹ The Department of Civil Protection and Emergency Management, Skógarhlíð 14, 105 Reykjavík, Iceland.

Corresponding author: Gro B. M. Pedersen (gro@hi.is)

Key Points:

- Near real-time photogrammetric monitoring of the 2021 Fagradalsfjall eruption
- Acquisition of an unprecedented temporal data set including volume, effusion rate, orthomosaics, thickness maps and thickness change maps
- After six months of eruption the lava covers 4.8 km², with a bulk volume of $\sim 1.5 \times 10^8$ m³ and mean effusion rate of ~ 9.5 m³/s

Abstract

The basaltic effusive eruption at Mt. Fagradalsfjall began on March 19, 2021, ending a 781-year hiatus on Reykjanes Peninsula, Iceland. By late September 2021, 32 near real-time photogrammetric surveys were completed using satellite and airborne images, usually processed within 3–6 hours. The results provide unprecedented temporal data sets of lava volume, thickness, and effusion rate. This enabled rapid assessment of eruption evolution and hazards to populated areas, important infrastructure, and tourist centers. The mean lava thickness exceeds 30 m, covers 4.8 km² and has a bulk volume of $150 \pm 3 \times 10^6$ m³. The March–September mean effusion rate is 9.5 ± 0.2 m³/s, ranging between 1–8 m³/s in March–April and increasing to 9–13 m³/s in May–September. This is uncommon for recent Icelandic eruptions, where the highest discharge usually occurs in the opening phase.

Plain Summary

On March 19, 2021, an eruption began at Mt. Fagradalsfjall after 781-years dormancy on the Reykjanes Peninsula, Iceland. To monitor and evaluate hazards of the eruption, satellite and airborne stereoisimages were processed and made publicly available on the same day as they were surveyed. The data were used to create 3D models of the lava and update the lava volume and growth rate. The resulting maps were used by disaster response teams to evaluate the risk of the lava flow to nearby infrastructure and to manage tourism in the vicinity of the eruption. On September 30, 2021, the new lava flow-field covered 4.8 km², was up to 124 m thick and had a mean thickness of 30 m, yielding a total bulk volume of 150 million m³. The mean discharge during the six months of the eruption was 9.5 m³/s, equivalent to filling one Olympic swimming pool every four minutes.

Key Words:

Effusive eruption, lava flows, near real-time monitoring, Fagradalsfjall, photogrammetry

1. Introduction

Effusion rates and volumes of lava flows are key eruption parameters necessary for evaluation of hazards posed by basaltic eruptions. Various methods exist to monitor and quantify near-real time effusion rate ranging from localized channel and tube estimates of instantaneous effusion rate to time-averaged discharge rate (TADR) based on satellite-based thermal data and synthetic aperture radar data (see Harris et al., 2007, Poland, 2014 and references therein). Photogrammetric methods are more recurrently and effectively applied in monitoring effusive eruptions (e.g., Dietterich et al. 2021). This study presents a significant achievement in full-scale monitoring of a lava field with photogrammetric methods that yielded daily to weekly 3-D models and effective near real-time processing and presentation of results. We show how near real-time photogrammetric monitoring in the Fagradalsfjall 2021 eruption provided key information necessary for evaluating hazards and delivering data products to Civil Protection, local police, and the public.

On March 19, 2021, an eruption started at Mt. Fagradalsfjall ending a 781-year eruption hiatus on the Reykjanes Peninsula, Iceland (Fig. 1). Fagradalsfjall is a broad hyaloclastite tuya located within an oblique spreading zone, characterized by volcanic systems and strike-slip faults that are associated with the Mid-Atlantic plate boundary (e.g., Klein et al., 1977; Gee, 1998; Clifton and Kattenhorn, 2006; Einarsson et al., 2020, Sæmundsson et al., 2020). Eruptions in Reykjanes occur from eruptive fissures, that may focus onto a single vent to form lava shields. When occurring under a glacier, these eruption types form cones, tindars or tuyas (e.g., Jones, 1969, Pedersen and Grosse, 2014). At least in the last four thousand years, volcanic activity on the Reykjanes Peninsula has been episodic, with multiple eruptions occurring over several hundred years followed by ~800–1000 years of quiescence. The last eruptive period ended in 1240 CE (Sæmundsson et al., 2020).

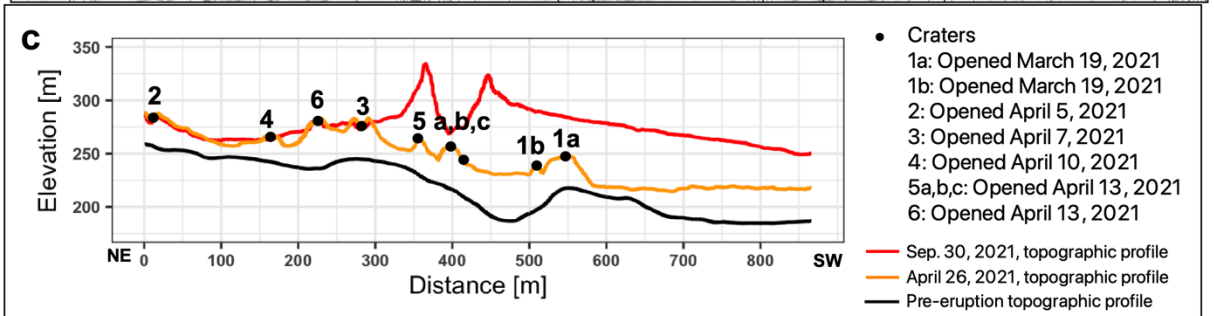
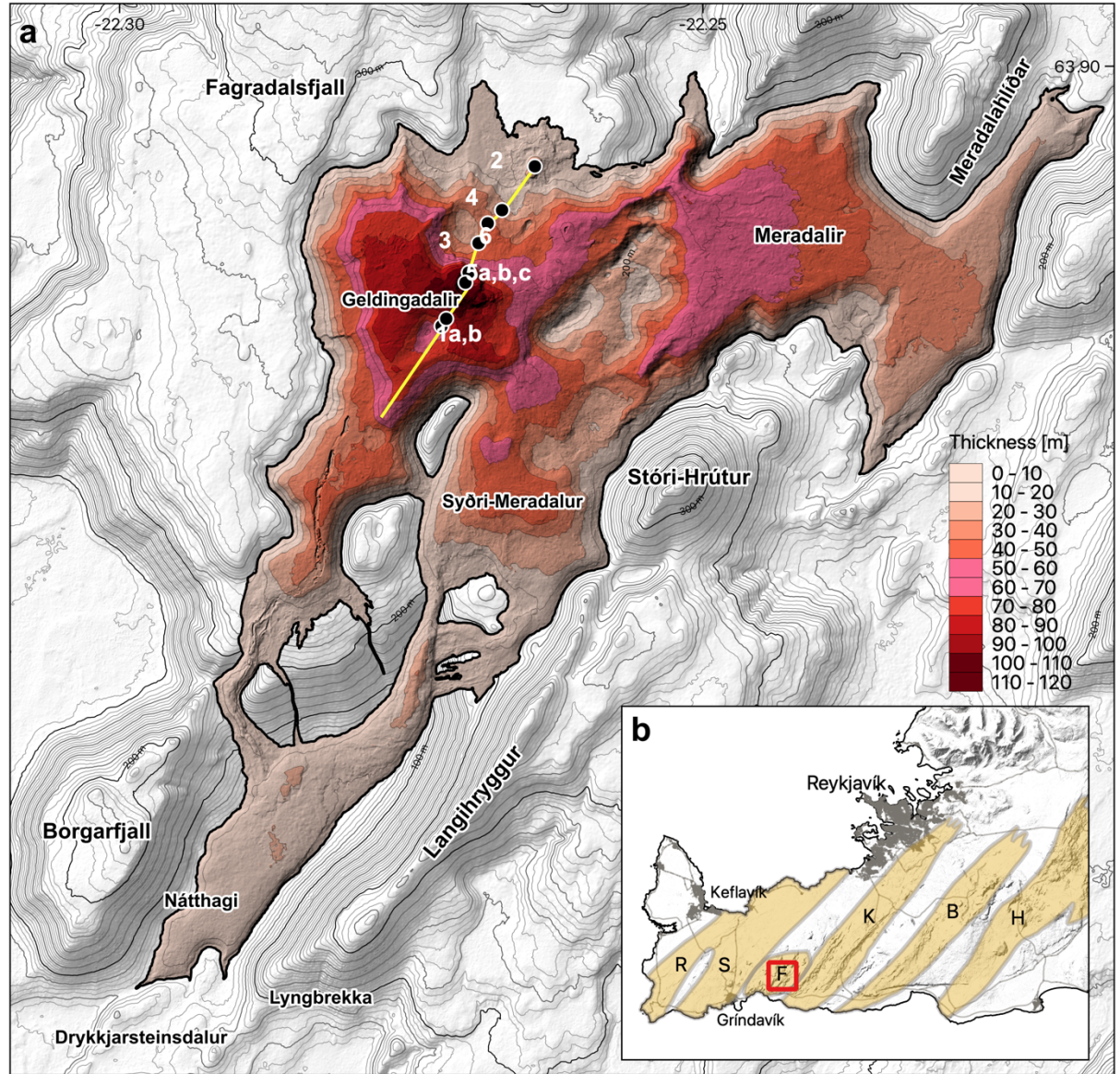


Figure 1 a) Thickness map of the erupted products in the Fagradalsfjall eruption by September 30, 2021. Vents are marked with a dot and numbered chronologically after opening time. Location of topographic profile in c) is marked as a yellow line. b) Map of the Reykjanes Peninsula. The red box indicates the area displayed in a). Densely populated areas are marked in gray. Volcanic systems (Sæmundsson and Sigurgeirsson, 2013) are marked with orange and denoted by capital letter according to their name; R: Reykjanes, S: Svartsengi, F: Fagradalsfjall, K: Krýsuvík, B: Brennisteinsfjöll, H: Hengill. c) Topographic profile along the vents from NE to SW (location see a).

2. Data and methods

The data used for near real-time monitoring of the Fagradalsfjall 2021 eruption consists mainly of aerial photographs and Pléiades stereoimages and by September 30, 2021, 32 surveys had been carried out (Supplement S1, Table S1). The processing of the Pléiades stereoimages is described in Gouhier et al. (submitted).

The airborne photogrammetric surveys of the eruption started on the morning of March 20, 2021, 11 hours after the eruption began. The bulk of surveys were done with the TF-BMW Partenavia P 68 Observer II survey aircraft operated by Garðaflug Corp (Table S1) with a Hasselblad A6D 100 MP medium-format camera with a 35 mm focal lens. Images were taken vertically at an altitude of 550–1800 m.a.s.l. with 75–90% overlap and image resolution of 7–30 cm. Up to 24 ground control points were placed around the lava flow-field and measured with a high-precision GNSS instrument (see Supplement S1).

The aerial photographs were processed in the software MicMac (Pierrot Deseiligny et al., 2011, Rupnik et al., 2017), following the semi-automated workflow of Belart et al. (2019), as well as in Agisoft Metashape (version 1.7.3) and Pix4D mapper (version 4.6.4) yielding the DEMs and orthomosaics. Each DEM was compared with a pre-eruption DEM and with the previous survey done, obtaining a thickness map and a thickness change map (Fig. 2 and 3).

Lava outlines were manually digitized from the orthomosaics. Volumes were calculated using the mean thickness of the erupted deposit multiplied by its area. The uncertainties of the volume were obtained using the Normalized Mean Absolute Deviation (Höhle and Höhle, 2009) of the stable areas surrounding the lavas, as proxy for the uncertainties of the thickness maps. The uncertainties of the TADR are described in Supplement S1.

3. Results

After each survey the data products: DEMs (2×2 m), orthomosaics (0.2×0.2 m to 0.5×0.5 m), thickness maps (2×2 m), and lava outlines were completed and made available, usually 3–6 hours after acquisition. A low-resolution 3D model was also released to the public (<https://www.ni.is/midlun/utgafa/thrividdarlikon/eldgos-vid-fagradalsfjall>) within 1–3 hours for visualization purposes. Thanks to the short latency of

data delivery the data products became important for the civil protection authorities. The orthomosaics and lava outlines were made available through an interactive map <http://atlas.lmi.is/mapview/?application=umbrotasja> and for geographic information systems through a Web Map Service (<https://gis.lmi.is/mapcache/reykjaneseldar/web-mercator/wms>). Figure S1 provides an example of data products delivered from each survey and table S2 provides results from each survey.

Here, we describe the evolution of the eruption, the erupted volume and TADR, as well as the lava flow-field development. Short-term fluctuations (minutes to hours) are not resolved by these measurements.

3.1. Fagradalsfjall eruption: Volume, discharge and lava field evolution

The eruption from March 19, 2021 to September 18, 2021 can be divided into five phases.

Phase 1 of the eruption (March 19 to April 5) began when a 180 m long fissure opened on March 19 around 20:30 in the Geldingadalir valley, which is located east of Mt. Fagradalsfjall (Fig. 1). Soon the eruption concentrated on two neighboring vents and the lava started infilling the valley (Fig. 2a). During this phase, the TADR ranged from 7.9 to 0.7 m³/s with a mean for the entire phase of 4.9±0.1 m³/s (Fig. 2b). The lava area increased to 0.33 km², while the mean thickness increased to 22 m reaching a lava volume of 7.1 × 10⁶ m³ before phase 2 started.

In phase 2 (April 5 to April 28) the active vent migrated (Fig. 1). Multiple eruption segments opened, starting on April 5, when two new fissure-segments opened 800 m northeast of the first fissure segments. Another fissure opened at midnight on April 7, another one on April 10 at and then again on April 13 when two new fissure segments opened. Each fissure segment concentrated into 1–2 circular vents, which over the following 10 days became inactive, except for southern the vents that developed from the April 13 fissure segments. Phase 2 had similar TADR as in phase 1 in the range 4.6–7.5 m³/s with the highest TADR observed just after new vent openings. The mean TADR in this period was 6.3±0.4 m³/s and the volume increased to 19.4 × 10⁶ m³. With the migration of active vent locations, lava started to flow into the valleys of Meradalir (April 5), Geldingadalir and Syðri-Meradalur (April 14) covering an area of 1.1 km² with a mean thickness of 16 m.

In phase 3 (April 28 to June 28) the vent activity stabilized at one location. Most of the time (May 2 to June 12) it exhibited cycles of short-term (ca. 8–9 minutes) pulsations. The TADR increased from 8.8 to a maximum of 13.0 m³/s with a phase mean of 11.4±0.5 m³/s. The “fill and spill” from one valley into another increased the area stepwise to 3.82 km² with mean thickness of 20.8 m yielding a volume of 79.8 × 10⁶ m³. The lava migrated to Nátthagi valley through Syðri-Meradalir (May 22) and through southern Geldingadalir (June 13).

Phase 4 (June 28 to September 2) was characterized by episodic activity with intense lava emplacement (ca. 12–24 hours) followed by inactive periods of similar length. Despite the episodic activity this period had only slightly lower TADR to phase 3 with a mean TADR for the whole phase of $11.0 \pm 0.4 \text{ m}^3/\text{s}$ ranging from 8.5 to $11.1 \text{ m}^3/\text{s}$ and the volume increased to $142.5 \times 10^6 \text{ m}^3$. The lava thickened to around 50 m northeast of the active crater due to episodic overflows and in Meradalir the lava thickened by $\sim 25 \text{ m}$ due to stacking and inflation.

The eruption's rhythm changed again in the phase 5 (September 2 to 18), when a week-long pause from September 2–11, was followed by week-long period of activity from September 11–18. The measured TADR was $12.2 \text{ m}^3/\text{s}$ for September 9–17. The mean TADR for phase 5 is $5.6 \pm 0.6 \text{ m}^3/\text{s}$ and the volume increased to $150.8 \times 10^6 \text{ m}^3$. Most of the deposition was in Geldingadalir, where a 10–15 m thick lava pond was established north-northwest of the active crater between September 11 to 15, that partly drained through an upwelling zone towards south and into Nátthagi from September 15 to 18. At the time of writing (November 18), no eruptive activity has been observed since September 18.

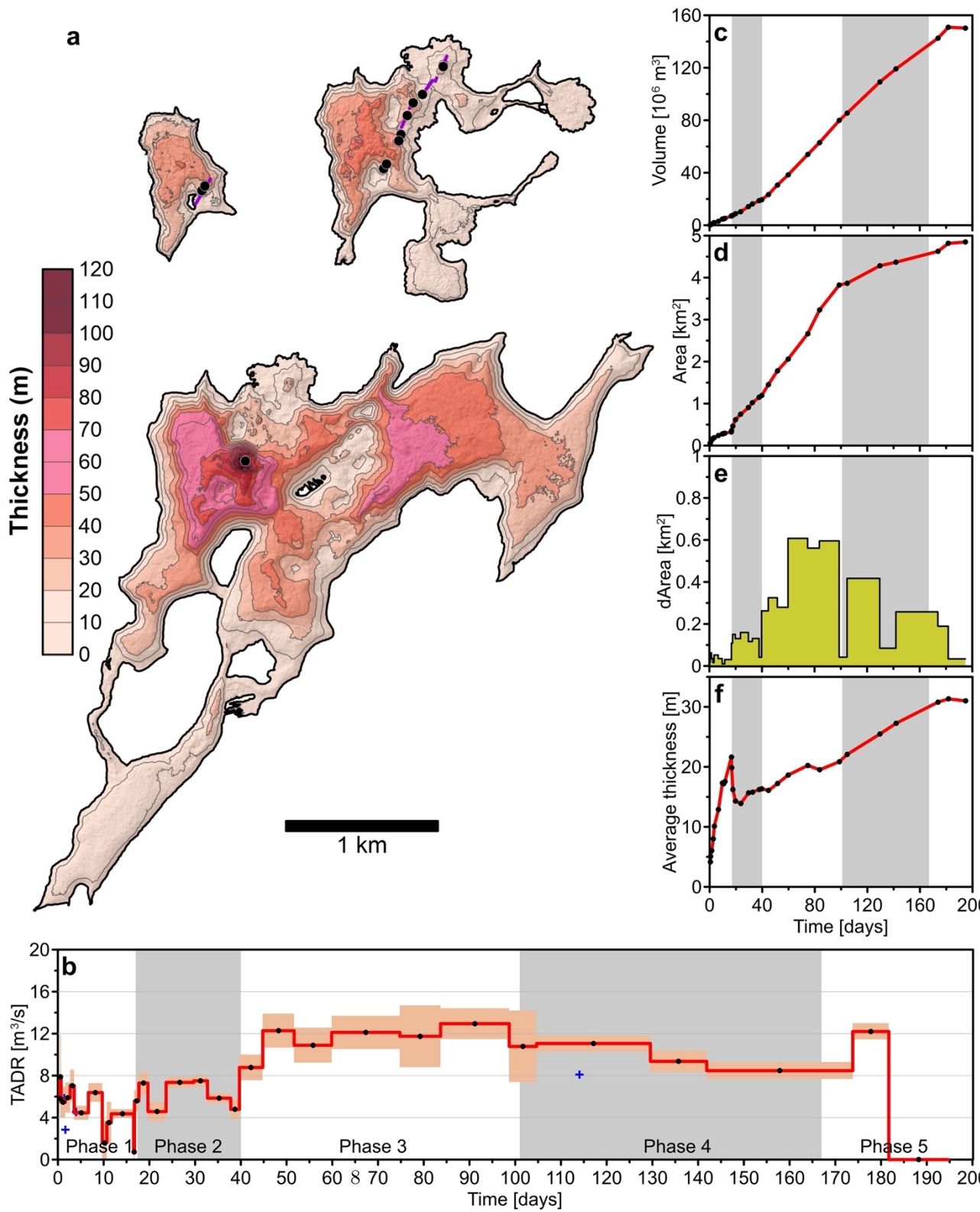


Figure 2 a) The thickness of erupted material by the end of phase 1 (April 5), end of phase 2 (April 26) and phase 4 (August 8, 2021). Purple line denotes initial fissure segment b–f) Eruption parameters of the Fagradalsfjall 2021 eruption showing the evolution of time-average discharge rate (TADR), volume, area, area change (dArea), and mean thickness. Orange boxes denote uncertainty in measurement. Blue crosses denote supporting TADR measurements (Supplement S2).

3.2. Lava transport systems and emplacement

Processes related to lava transport and emplacement could be studied through thickness change maps (Fig. 3a–c) such as breakouts, inflation, lava stacking, pond formation, channel changes, deflation, cooling and contraction as well as vent changes. Especially, monitoring of inflation within valleys that were likely to spill into lower lying terrain was important since some sections of popular hiking trails were located below lava-filled valleys.

Despite the relatively stable effusion rate in phase 3 and 4 (Fig. 2), the braided lava pathways and the lava advancement were complex and variable as the lava filled and spilled from one valley into another. Short-term prediction of the timing of overflow from one valley to another provided challenges and thus monitoring the changes in the lava transport system and lava deposition in different valleys became important. The lava pathways were strongly controlled by the topography and mainly confined to the valleys and the steep slopes connecting them. However, since the valley systems consisted of multiple valleys east and south of the active vents the lava pathways were not uniformly filling up the valleys but switching from one valley to another. One way to monitor these changes and estimate the variability was to investigate the volume changes in different zones and vent distances (at 100 m interval) based on the thickness change maps. For each zone we could calculate the V/t reflecting the volume deposited for a given period at a specific vent distance. This allows us to display the changes in lava transport and deposition in between these zones and distances over time (Fig. 3d).

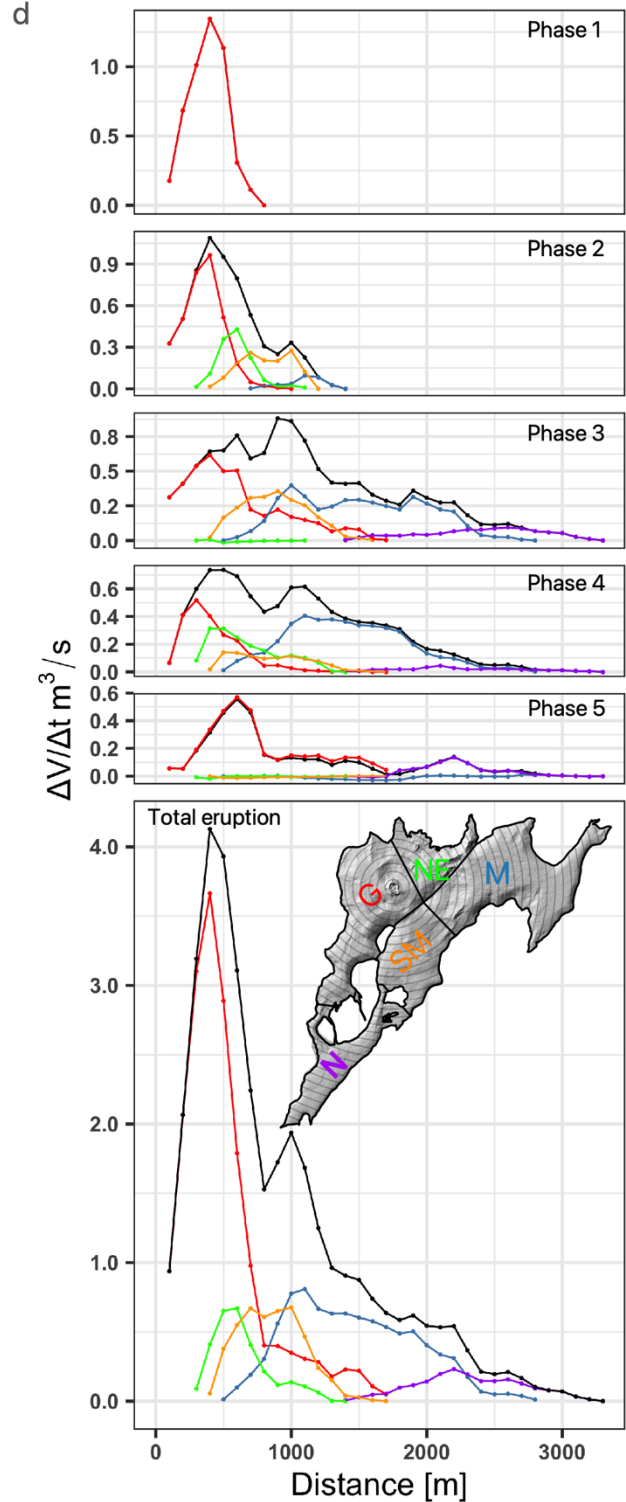
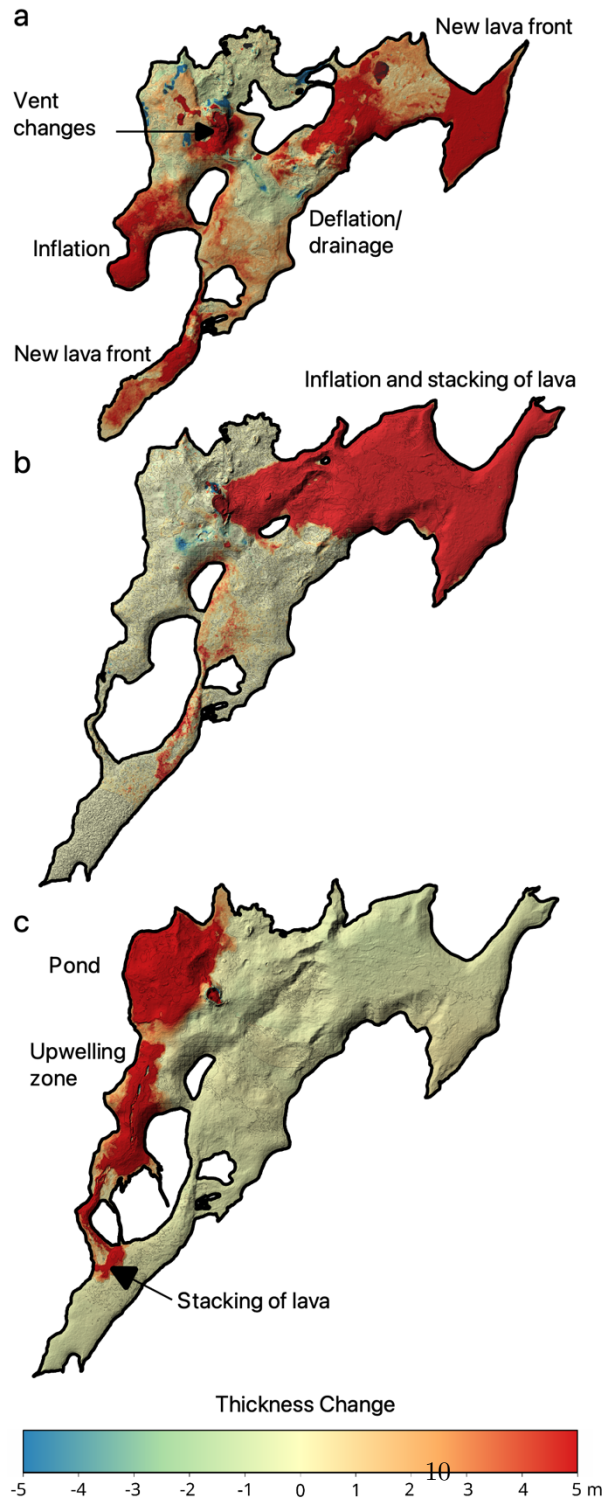


Figure 3 Thickness change map from a) June 2–11 b) July 2–27 and c) September 9–17 showing observable emplacement processes. d) V/t as a function of vent distance for each phase in five zones (see inset for location); G: Geldingadalir, M: Meradalir, SM: Syðri-Meradalur, N: Nátthagi and NE: the plateau northeast of the vent. The black line is the total V/t for all five zones as a function of vent distance. In phase 1 all lava was deposited in Geldingadalir and thus the total V/t is equal to the V/t for Geldingadalir. The lower panel shows the total deposition from March to September between zones as a function of vent distance.

The lava deposition as a function of vent distance changed markedly over time. In phase 1 all lava was emplaced within Geldingadalir; and, in phase 2, as new vents opened on the northeast plateau, lava migrated into Meradalir and Syðri-Meradalur. In phase 3, the lava field expanded to its current maximum extent, reaching 3.3 km from the vent by having lava ponds acting as reservoirs for the transport system (Fig. 3d). This lava transport system closed during phase 4, when the continuous lava effusion was replaced by episodic activity responsible for large overflows and significant stacking in the vent region. Stacking and inflation was continued in Meradalir, where the lava reached a distance of 2.8 km from the vent. Thus, despite the long-term TADR in phases 3 and 4 was similar (Fig. 2), the difference between continuous and episodic activity at the vent had a major impact on the lava transport system and the ability of the lava field to expand. In phase 5, most lava emplacement was within a 1 km radius of the active vent but reached 2.7 km in mid-September after the drainage of a pond northwest of the crater (Fig. 3c). Between surveys this variation of lava deposition between zones amounted to as much as $10 \text{ m}^3/\text{s}$ for Geldingadalir and Meradalir, $5 \text{ m}^3/\text{s}$ for Syðri-Meradalur and the Northeast plateau and $3 \text{ m}^3/\text{s}$ for Nátthagi. Thus, despite a stable TADR, the local effusion into individual valleys varied significantly between surveys providing a great challenge for forecasting the timing of lava spilling from one valley to another.

4. Discussion

Satellite and airborne photogrammetry provided flexible methods for near real-time monitoring of volume and TADR on a daily to weekly basis for Icelandic conditions, where low vegetation and very changeable weather prevails. Airplane surveys were possible for cloud cover down to 550 m.a.s.l and could be deployed quickly since the flight to the eruption only takes 10 minutes from Reykjavík Airport (RVK). The acquisitions were mainly limited by the low cloud, and occasionally by lack of available aircraft.

The data products (orthomosaics, DEM, lava outline, thickness maps, thickness change maps and volume and TADR estimates) provided critical information for disaster response and for the scientific community. The volume and TADR were used to evaluate the status of the eruption and as input parameters together with the thickness maps for lava flow simulation. The orthomosaics and lava outlines were important to responders providing base maps for infrastructure, planning, rescue missions, and for tourists visiting the eruption.

The effusion rate evolution for basaltic eruptions provides important insights to increase understanding of the source of the magma and the conduit properties. Different trends in effusion rate evolution have been classified into types and linked to specific plumbing system dynamics (Harris et al., 2000, 2011, Araveno et al., 2020). Type I is characterized by a phase of high initial effusion followed by an extended phase of waning effusion, which has been interpreted as a tapping of a pressurized reservoir (Wadge et al., 1981) and efficient magma ascent in early stages (Araveno et al., 2020). Type II has a low, near-constant effusion rate and has been related to low values of overpressure (5–10 MPa), consistent with overflow in a non-pressurized system (Harris et al. 2000, Araveno et al., 2020). In type III eruptions, the effusion rate increases with time and has been suggested to be linked with ascent of a magma batch, pushing a volume of degassed magma ahead (Harris et al., 2011). However, this trend has also been linked to conduit erosion caused by high erosion coefficients, high initial overpressures, and/or large magma reservoirs, that in its extreme case may lead to a sudden overpressure drop and eruption shutdown caused by high effusion rate and magma withdrawal (Araveno et al., 2020). The last type is type IV, which shows highly pulsating effusion rate and has been related to ascent of multiple batches of magma (Harris et al., 2011).

The Fagradalsfjall 2021 eruption started with low and stable effusion rate between 4–8 m³/s in phase 1–2 (Fig. 2) and initially had the characteristics of a type II eruption. However, in phase 3–4 the effusion rate increased to 8–13 m³/s changing the characteristics to resemble a type III eruption, whilst in phase 5 the TADR had pulsating characteristics similar to type IV but lasted only for a month. The low initial effusion rate at Fagradalsfjall is between 30 and 2500 times smaller than other recorded Icelandic eruptions in the last 75 years (Gudmundsson et al., 2004, 2012, Jude-Eton et al., 2012, Hreinsdóttir et al., 2014, Pedersen et al., 2017, 2018, Thorarinsson, 1964, 1967). When normalizing the initial effusion rate to the mean output rate (Harris et al. 2007) of each eruption, it becomes clear that it is not only a low initial effusion rate that is unusual, but the evolution of the effusion rate at Fagradalsfjall, which is unlike any observations from previous recent Icelandic eruptions (Fig. 4).

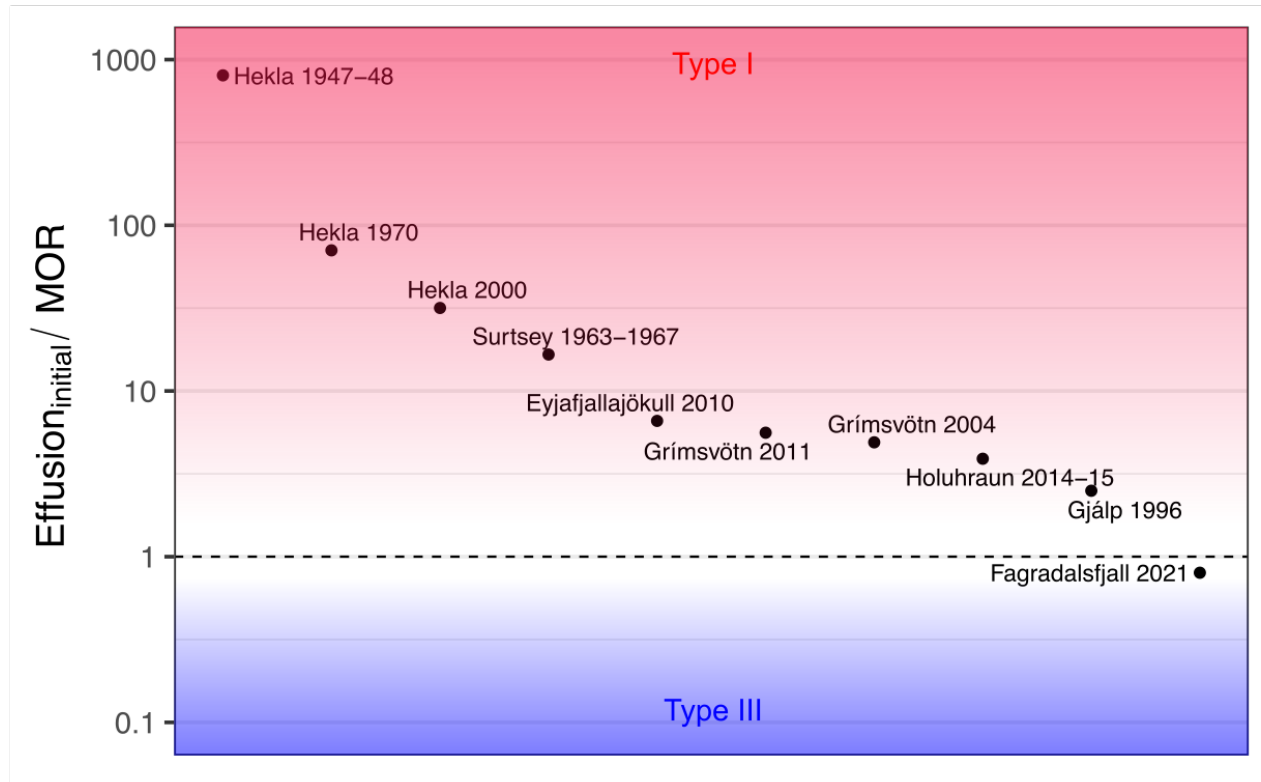


Figure 4 Fagradalsfjall effusion characteristics described by the ratio of initial effusion rate $\text{Effusion}_{\text{initial}}$ divided by the Mean Output Rate, MOR (Harris et al., 2007) compared to other recent Icelandic eruptions (Gudmundsson et al., 2004, 2012, Jude-Eton et al., 2012, Hreinsdóttir et al., 2014, Pedersen et al., 2017, 2018, Thorarinsson, 1964,1967). Note the y-axis is logarithmic. Fagradalsfjall 2021 is clearly an outlier with a ratio below 1, while all other eruptions plot above 1. The effusion rate evolution of types I and III from Harris et al (2000, 2011) has been indicated in red and blue. Type II should ideally plot along the dashed line, while the pulsating nature of type IV could plot everywhere in the plot.

For the first time we observe an eruption that primarily has characteristics of a type III eruption, while recent Icelandic eruptions show characteristics that resemble type I eruptions. Based on the interpretation of type I eruptions, it makes sense that eruptions in Hekla, Grímsvötn and Bárðarbunga (Holuhraun 2014–2015) all show effusion rate evolution controlled by pressurized reservoirs, since these volcanic systems show evidence of having magma chambers (e.g.,

Ofeigsson et al., 2011, Geirsson et al., 2012, Hreinsdóttir et al., 2014, Gudmundsson et al., 2016). Less information exists for the Vestmannaeyjar volcanic system responsible for the Surtsey 1963–1967 eruption, but based on the available data (Thorarinsson, 1964), the effusion rate evolution suggests that Fagradalsfjall is unlike this eruption as well.

The evolution of the effusion rate of type III eruptions has been linked to the ascent of a single magma batch, pushing a volume of degassed magma ahead (Harris et al., 2011, Steffke et al., 2011). Interestingly, geochemical evidence suggests that in phase 1–2 the magma plumbing system gradually changed from being fed from a depleted shallow mantle source to being fed by more enriched discrete melts from greater depth (Marshall et al., 2021). Nevertheless, this gradual geochemical change happened during the first 40 days of the eruption, where the TADR is stable and the increase in TADR happen around day 50. However, during phase 2, new vents opened at locations which were 60 m above the initial vents in Geldingadalir (Fig. 1) suggesting an increase in pressure during this time (in the order of 1–1.5 MPa based on higher lithostatic load corresponding to 60 m increase in elevation of vents). By the end of phase 2, the vents at the higher elevations had shut off and the effusion from vent 5, which is located in similar elevation as vent 1a,b increased from 7 to 13 m³/s in phase 3, while displaying fire fountain activity.

The delay between the geochemical change and the increased effusion is intriguing. In the 2018 Kilauea eruption the increase in effusion started within a day of an observed change to more mafic magma increasing the effusion from 6.5 m³/s to 110 m³/s (Gansecki et al., 2019, Dietterich et al., 2021). Furthermore, this change was associated with observed deformation and earthquake activity. Thus, there was a clear link between a change in geochemistry and a substantial increase in effusion.

If the effusion increase in Fagradalsfjall is related to ascent of a magma batch pushing a degassed magma ahead (which would be 20×10^6 m³ based on the erupted bulk volume estimates at day 40), then it is clear that it is a more subtle process compared to the 2018 Kilauea eruption, potentially involving lower overpressure and slower increase in effusion.

Another possible model used to explain increase in effusion with thermal erosion. The eruption in phase 1–2 displayed type II characteristics consistent with overflow in a non-pressurized system. The effusion rate and the successive vent openings suggest that the system was not highly pressurized. Over time the heating of the conduit walls enabled sufficient thermal erosion to increase the effusion rate, which for a cylindrical conduit is proportional to r^4 , where r is radius (e.g., Turcotte and Schubert, 2002). This process may have been enhanced by the increased temperature of the magma due to an increase in MgO from 8.8–9.7% (Marshall et al., 2021). We consider this conduit-controlled flow a plausible model for Fagradalsfjall because it explains the sharp contrast with the behavior to other Icelandic eruptions (e.g., Hekla, Grímsvötn and Bárðarbunga) where pressure in a magma chamber is considered the main control of

flow (e.g., Hreinsdóttir et al., 2014).

5. Conclusions

Near real-time photogrammetric monitoring of the eruption at Fagradalsfjall 2021 was performed using a combination of satellite and airborne stereoimages as a part of the response to the event. This provided essential eruption parameters such as volume and effusion rate, as well as the maps distributed to the public, the Civil Protection, rescue teams, and the tourism industry.

By September 30, 2021, 32 surveys have been performed. Currently, the lava flow-field covers 4.8 km² and the estimated bulk volume (including vesicles and macroscale porosity) is 150×10^6 m³, yielding a mean effusion rate (from the beginning of the eruption start) of 9.5 ± 0.2 m³/s.

The lava pathways and lava advancement were very complex and changeable as the lava filled and spilled from one valley into another and short-term prediction of the timing of overflow from one valley to another proved challenging. Analysis of thickness maps and thickness change maps show that the lava transport into different valleys varied up to 10 m³/s between surveys as lava transport rapidly switched between one valley to another.

Compared to recent Icelandic eruptions, the evolution of the effusion rate is very unusual, having a very low and stable effusion in phase 1–2 and increasing effusion in phase 3. This behavior may be due to widening of the conduit by thermal erosion with time, and not controlled by magma chamber pressure as is most common in the volcanic zones of Iceland.

Acknowledgements

The data from airborne surveys will be available on <https://zenodo.org/> and data from Pléiades will be available on <https://www.theia-land.fr/en/product/pleiades/>. The processed data is currently available in the Supporting Information for the purposes of review.

We would like to thank our pilots Ú. Henningsson, K. Kárason, K. Halldórsdóttir, G. Árnason, J.Sverrisson, the Icelandic Coast Guard and Iceland Aviation Service for their commitment to carry out flights. The authors would like to acknowledge the Icelandic Research fund, Grant No. 206755-052, the Fulbright–NSF Arctic Scholar program, NSF RAPID program and the French Space Agency (CNES) for their support. Pléiades images were provided under the CIEST² (CNES) initiative during the first 10 days of the eruption and through the Icelandic Volcanoes Supersite project supported by the Committee on Earth Observing Satellites (image Pléiades©CNES2021, distribution AIR-BUS DS).

References

Aravena, A., Cioni, R., Coppola, D., Vitturi, M. de' M., Neri, A., Pistolesi, M., & Ripepe, M. (2020). Effusion Rate Evolution During Small-Volume Basaltic Eruptions: Insights From Numerical Modeling.

Journal of Geophysical Research: Solid Earth, 125(6), e2019JB019301.
<https://doi.org/10.1029/2019JB019301>

Belart, J. M. C., Magnússon, E., Berthier, E., Pálsson, F., Aðalgeirsdóttir, G., and Jóhannesson, T. (2019). The geodetic mass balance of Eyjafjallajökull ice cap for 1945-2014: processing guidelines and relation to climate. *J. Glaciol.* 65, 395–409. doi: 10.1017/jog.2019.16

Clifton, A. E., & Kattenhorn, S. A. (2006). Structural architecture of a highly oblique divergent plate boundary segment. *Tectonophysics*, 419(1), 27–40. <https://doi.org/10.1016/j.tecto.2006.03.016>

Dietterich, H. R., Diefenbach, A. K., Soule, S. A., Zoeller, M. H., Patrick, M. P., Major, J. J., & Lundgren, P. R. (2021). Lava effusion rate evolution and erupted volume during the 2018 Kilauea lower East Rift Zone eruption. *Bulletin of Volcanology*, 83(4), 25. <https://doi.org/10.1007/s00445-021-01443-6>

Einarsson, P., Hjartardóttir, Á. R., Imsland, P., Hreinsdóttir, S. (2020). The structure of seismogenic strike-slip faults in the eastern part of the Reykjanes Peninsula oblique rift, SW Iceland. *Journal of Volcanology and Geothermal Research* 106372, doi:10.1016/j.jvolgeores.2018.04.029.

Gansecki, C., Lee, R. L., Shea, T., Lundblad, S. P., Hon, K., & Parcheta, C. (2019). The tangled tale of Kilauea's 2018 eruption as told by geochemical monitoring. *Science*, 366(6470). <https://doi.org/10.1126/science.aaz0147>

Gardelle J., Berthier E., Arnaud Y. & Kääb, A. (2013) Region-wide glacier mass balances over the Pamir - Karakoram - Himalaya during 1999-2011. *The Cryosphere*, 7, 1263-1286, doi: 10.5194/tc-7-1263-2013.

Gee, M. A. M. (1998). *Volcanology and geochemistry of Reykjanes Peninsula: Plume-mid-ocean ridge interaction*. [PhD]. University of London.

Geirsson, H., LaFemina, P., Árnadóttir, T., Sturkell, E., Sigmundsson, F., Travis, M., Schmidt, P., Lund, B., Hreinsdóttir, S., & Bennett, R. (2012). Volcano deformation at active plate boundaries: Deep magma accumulation at Hekla volcano and plate boundary deformation in south Iceland. *Journal of Geophysical Research: Solid Earth*, 117(B11). <https://doi.org/10.1029/2012JB009400>

Gouhier, M., Pinel, V., Belart, J. DeMichele, M. Proy, C., Tinel, C., Berthier, E., Guéhenneux, Y., Gudmundsson, M. T., Óskarsson B. V., Gremion, S., Raucoules, D., Valade, S., Massimetti, F. Oddsson, B. (submitted). CNES-ESA satellite contribution to the operational monitoring of volcanic activity: The 2021 Icelandic eruption of Mt. Fagradalsfjall. *Journal of Applied Volcanology*

Gudmundsson, M.T., Högnadóttir, P., Kristinsson, A.B., Gudbjörnsson, S. (2007). Geothermal activity in the subglacial Katla caldera, Iceland, 1999-2005, studied with radar altimetry. *Annals of Glaciology*, 45, 66-72, doi.org/10.3189/172756407782282444.

Gudmundsson, M.T., K. Jónsdóttir, A. Hooper, E.P. Holohan, S.A. Halldórsson, B.G. Ófeigsson, S. Cesca, K.S. Vogfjörð, F. Sigmundsson, Th. Högnadóttir, P. Einarsson, O. Sigmarsson, A.H. Jarosch, K. Jónasson, E. Magnússon, S. Hreinsdóttir, M. Bagnardi, M.M. Parks, V. Hjörleifsdóttir, F. Pálsson, T.R. Walter, M.P.J. Schöpfer, S. Heimann, H.I. Reynolds, S. Dumont, E. Bali, G.H. Gudfinnsson, T. Dahm, M.J. Roberts, M. Hensch, J. M.C. Belart, K. Spaans, S. Jakobsson, G.B. Gudmundsson, H.M. Fridriksdóttir, V. Drouin, T. Dürig, G. Adalgeirsdóttir, M.S. Riishuus, G.B.M. Pedersen, T. van Boeckel. B. Oddsson, M.A. Pfeffer, S. Barsotti, B. Bergsson, A. Donovan, M.R. Burton, A. Aiuppa. (2016). Gradual caldera collapse at Bárðarbunga volcano, Iceland regulated by lateral magma outflow. *Science* 353, aaf8988. DOI: 10.1126/science.aaf8988.

Gudmundsson, M. T., Sigmundsson, F., Björnsson, H., & Högnadóttir, T. (2004). The 1996 eruption at Gjalp, Vatnajökull ice cap, Iceland: Efficiency of heat transfer, ice deformation and subglacial water pressure. *Bulletin of Volcanology*, 66(1), 46–65. <https://doi.org/10.1007/s00445-003-0295-9>

Gudmundsson, M.T., Thordarson, T., Höskuldsson, Á., Larsen G., Björnsson, H., Prata, A.J., Oddsson, B., Magnússon, E., Högnadóttir, T., Pedersen, G.N., Hayward, C.L., Stevenson, J.A., Jónsdóttir, I. (2012). Ash generation and distribution from the April-May 2010 eruption of Eyjafjallajökull, Iceland. *Scientific Reports*. 2, 572; DOI:10.1038/srep00572

Harris, A. J. L., Dehn, J., & Calvari, S. (2007). Lava effusion rate definition and measurement: A review. *Bulletin of Volcanology*, 70(1), 1. <https://doi.org/10.1007/s00445-007-0120-y>

Harris, A. J. L., Murray, J. B., Aries, S. E., Davies, M. A., Flynn, L. P., Wooster, M. J., Wright, R., & Rothery, D. A. (2000). Effusion rate trends at Etna and Krafla and their implications for eruptive mechanisms. *Journal of Volcanology and Geothermal Research*, 102(3), 237–269. [https://doi.org/10.1016/S0377-0273\(00\)00190-6](https://doi.org/10.1016/S0377-0273(00)00190-6)

Harris, A., Steffke, A., Calvari, S., & Spampinato, L. (2011). Thirty years of satellite-derived lava discharge rates at Etna: Implications for steady volumetric output. *Journal of Geophysical Research: Solid Earth*, 116(B8). <https://doi.org/10.1029/2011JB008237>

Hreinsdóttir, S., Sigmundsson, F., Roberts, M. J., Björnsson, H., Grapenthin, R., Arason, Th., Árnadóttir, T., Hólmjárn, J., Geirsson, H., Bennett, R. A., Gudmundsson, M. T., Oddsson, B., Ófeigsson, B. G., Villemin, T., Jónsson, T., Sturkell, E., Höskuldsson, A., Larsen, G., Thordarson, T., & Óladóttir, B. A. (2014). Volcanic plume height correlated with magma-pressure change at Grímsvötn Volcano, Iceland. *Nature Geoscience*, 7, 214–218. <https://doi.org/10.1038/ngeo2044>

Höhle, J. and Höhle, M. (2009). Accuracy assessment of digital elevation models by means of robust statistical methods, *ISPRS J. Photogramm. Remote Sens.*, 64, 398–406, doi:10.1016/j.isprsjprs.2009.02.003.

- Jones, J. G. (1969). Intraglacial volcanoes of the Laugarvatn region, southwest Iceland—I. Quarterly Journal of the Geological Society, 124(1–4), 197–211. <https://doi.org/10.1144/gsjgs.124.1.0197>
- Jude-Eton, T.C., Thordarson, Th., Gudmundsson, M.T., Oddsson, B. (2012). Dynamics, stratigraphy and proximal dispersal of supraglacial tephra during the ice-confined 2004 eruption at Grímsvötn volcano, Iceland. *Bull. Volc.*, 74, 1057–1082. DOI: 10.1007/s00445-012-0583-3.
- Klein, F. W., Einarsson, P., & Wyss, M. (1977). The Reykjanes Peninsula, Iceland, earthquake swarm of September 1972 and its tectonic significance. *Journal of Geophysical Research (1896-1977)*, 82(5), 865–888. <https://doi.org/10.1029/JB082i005p00865>
- Marshall, E. W., Rasmussen, M. B., Halldorsson, S. A., Matthews, S., Ranta, E., Sigmarsson, O., Robin, J. G., Bali, E., Caracciolo, A., Gudfinnsson, G. H. and Mibei, G. K. (2021) Rapid geochemical evolution of the mantle-sourced Fagradalsfjall eruption, Iceland. AGU Fall meeting, New Orleans, USA
- Nuth, C. and Kääb, A. (2011). Co-registration and bias corrections of satellite elevation data sets for quantifying glacier thickness change. *The Cryosphere*, 5, 271–290, <https://doi.org/10.5194/tc-5-271-2011>.
- Ofeigsson, B. G., Hooper, A., Sigmundsson, F., Sturkell, E., & Grapenthin, R. (2011). Deep magma storage at Hekla volcano, Iceland, revealed by InSAR time series analysis. *Journal of Geophysical Research: Solid Earth*, 116(B5). <https://doi.org/10.1029/2010JB007576>
- Óskarsson, B. V.; Jónasson, K.; Valsson, G. & Belart, J. M. C. (2020). Erosion and sedimentation in Surtsey island quantified from new DEMs, Surtsey Research, 14, 63–77.
- Pedersen, G. B. M., Belart, J. M. C., Magnússon, E., Vilmundardóttir, O. K., Kizel, F., Sigurmundsson, F. S., Gísladóttir, G., & Benediktsson, J. A. (2018). Hekla Volcano, Iceland, in the 20th Century: Lava Volumes, Production Rates, and Effusion Rates. *Geophysical Research Letters*, 45(4), 1805–1813. <https://doi.org/10.1002/2017GL076887>
- Pedersen, G. B. M., & Grosse, P. (2014). Morphometry of subaerial shield volcanoes and glaciovolcanoes from Reykjanes Peninsula, Iceland: Effects of eruption environment. *Journal of Volcanology and Geothermal Research*, 282, 115–133. <https://doi.org/10.1016/j.jvolgeores.2014.06.008>
- Pedersen, G. B. M., Höskuldsson, A., Dürig, T., Thordarson, T., Jónsdóttir, I., Riishuus, M. S., Óskarsson, B. V., Dumont, S., Magnusson, E., Gudmundsson, M. T., Sigmundsson, F., Drouin, V. J. P. B., Gallagher, C., Askew, R., Gudnason, J., Moreland, W. M., Nikkola, P., Reynolds, H. I., & Schmith, J. (2017). Lava field evolution and emplacement dynamics of the 2014–2015 basaltic fissure eruption at Holuhraun, Iceland. *Journal of Volcanology and Geothermal Research*, 340, 155–169. <https://doi.org/10.1016/j.jvolgeores.2017.02.027>

- Pierrot Deseilligny, M., and Clery, I. (2011). Apero, an open source bundle adjustment software for automatic calibration and orientation of set of images. *Int. Arch. Photogr. Remote Sens. Spat. Inform. Sci.* 3816, 269–276. doi: 10.5194/isprsarchives-XXXVIII-5-W16-269-2011
- Poland, M. P. (2014). Time-averaged discharge rate of subaerial lava at Kīlauea Volcano, Hawai'i, measured from TanDEM-X interferometry: Implications for magma supply and storage during 2011–2013. *Journal of Geophysical Research: Solid Earth*, 119(7), 5464–5481. <https://doi.org/10.1002/2014JB011132>
- Porter, C., Morin, P., Howat, I., Noh, M.-J., Bates, B., Peterman, K., et al. (2018). *ArcticDEM*. Harvard Dataverse, V1. Polar Geospatial Center, University of Minnesota. doi: 10.7910/DVN/OHHUKH
- Rupnik, E., Daakir, M., and Pierrot Deseilligny, M. (2017). MicMac - a free, open-source solution for photogrammetry. *Open Geospatial Data Softw. Stand.* 2:14. doi: 10.1186/s40965-017-0027-2
- Sæmundsson, K., & Sigurgeirsson, M. Á. (2013). Reykjaneskagi. In J. Sólnes, F. Sigmundsson, & B. Bessason (Eds.), *Náttúruvá* (pp. 379–401). Viðlagatrygging Íslands / Háskólaútgáfa.
- Sæmundsson, K., Sigurgeirsson, M. Á., & Friðleifsson, G. Ó. (2020). Geology and structure of the Reykjanes volcanic system, Iceland. *Journal of Volcanology and Geothermal Research*, 391, 106501. <https://doi.org/10.1016/j.jvolgeores.2018.11.022>
- Shean, D. E., Alexandrov, O., Moratto, Z. M., Smith, B. E., Joughin, I. R., Porter, C., Morin, P. (2016). An automated, open-source pipeline for mass production of digital elevation models (DEMs) from very-high resolution commercial stereo satellite imagery, ISPRS Journal of Photogrammetry and Remote Sensing, Vol. 116, pp 101-117, <https://doi.org/10.1016/j.isprsjprs.2016.03.012>.
- Steffke, A. M., Harris, A. J. L., Burton, M., Caltabiano, T., & Salerno, G. G. (2011). Coupled use of COSPEC and satellite measurements to define the volumetric balance during effusive eruptions at Mt. Etna, Italy. *Journal of Volcanology and Geothermal Research*, 205(1), 47–53. <https://doi.org/10.1016/j.jvolgeores.2010.06.004>
- Sørensen, E. V. & Dueholm, M. (2018). Analytical procedures for 3D mapping at the Photogeological Laboratory of the Geological Survey of Denmark and Greenland, Geological Survey of Denmark and Greenland Bulletin, 41, 99-104. DOI:<https://doi.org/10.34194/geusb.v41.4353>.
- Thorarinsson, S., Einarsson T, Sigvaldason G, Elisson G (1964) The submarine eruption off the Vestmann islands 1963-64 - A preliminary report. *Bulletin Volcanologique* 27:435–445. <https://doi.org/10.1007/BF02597544>
- Thorarinsson, S. (1968) *Heklueldar* (In Icelandic: the Hekla fires).. Sögufélag. 185 pp.

Turcotte, D.L., Schubert, G. 2002. *Geodynamics*, 2nd Ed. Cambridge, University Press. 456 pp.

Wadge, G. (1981). The variation of magma discharge during basaltic eruptions. *Journal of Volcanology and Geothermal Research*, 11(2), 139–168. [https://doi.org/10.1016/0377-0273\(81\)90020-2](https://doi.org/10.1016/0377-0273(81)90020-2)